

1 Article

2 **Warming effects at cold–dry forests: positive or**
3 **negative balance of trade? The case of *Pinus***
4 ***sylvestris* in the Siberian forest steppe**

5 **Tatiana A. Shestakova**^{1,2,*}, **Jordi Voltas**¹, **Matthias Saurer**³, **Rolf T. W. Siegwolf**⁴ and **Alexander**
6 **V. Kirdyanov**^{2,5}

7 ¹ Department of Crop and Forest Sciences – AGROTECNIO Center, University of Lleida, Avda. Rovira
8 Roure 191, 25198 Lleida, Spain; tasha.work24@gmail.com (T.A.S.); jvoltas@pvcf.udl.cat (J.V.)

9 ² Siberian Federal University, st. L. Prushinskoy 2, 660075 Krasnoyarsk, Russia

10 ³ Swiss Federal Institute for Forest, Snow and Landscape Research (WSL), Zürcherstrasse 111, 8903
11 Birmensdorf, Switzerland; matthias.saurer@wsl.ch

12 ⁴ Laboratory of Atmospheric Chemistry, Paul Scherrer Institute (PSI), 5232 Villigen, Switzerland;
13 rolf.siegwolf@psi.ch

14 ⁵ Sukachev Institute of Forest, Akademgorodok 50/28, 660036 Krasnoyarsk, Russia; kirdyanov@ksc.krasn.ru

15

16 * Correspondence: tasha.work24@gmail.com; Tel.: +34-973-702522

17 Academic Editor:

18 Received: date; Accepted: date; Published: date

19 **Abstract:** Understanding the impact of climate change on droughted forests is a critical issue. We
20 investigated ring-width and stable isotopes ($\Delta^{13}\text{C}$ and $\delta^{18}\text{O}$) in two *Pinus sylvestris* stands of the cold-
21 dry Central Siberian forest–steppe growing under contrasting climatic trends over the last 75 years.
22 Despite overall regional warming, there was increasing precipitation during the growing period at
23 the southern site (MIN) but increasing water deficit (WD) at the northern site (BER). Intrinsic water-
24 use efficiency (WUE_i) increased at both sites (*ca.* 22%) in response to warming and rising
25 atmospheric CO_2 . However, the steady increase in WUE_i was accompanied by divergent growth
26 patterns since 1980: increasing basal area increment (BAI) in MIN (slope = $0.102 \text{ cm}^2 \text{ year}^{-2}$) and
27 decreasing BAI in BER (slope = $-0.129 \text{ cm}^2 \text{ year}^{-2}$). This outcome suggests that increasing
28 precipitation, mediated by CO_2 effects, promoted growth in MIN, whereas enhanced drought stress
29 led to decreased carbon gain and productivity in BER. When compared to warm-dry stands of
30 eastern Spain, the WUE_i dependence on WD was 3-fold greater in Siberia. Conversely, BAI was
31 more affected by the relative impact of water stress within each region. These results suggest
32 contrasting future trajectories of *P. sylvestris* forests in cold-dry areas.

33 **Keywords:** climate warming, dendroecology, drought stress, forest steppe, Scots pine, Central
34 Siberia, stable isotopes, tree rings

35

36 **1. Introduction**

37 Scots pine (*Pinus sylvestris* L.) is the world’s most widespread conifer as it can be found
38 throughout Eurasia from the western Mediterranean to the Russian Far East. Such vast distribution
39 encompasses a broad array of climates, including the frequent and severe summer droughts of
40 southern Iberian Peninsula and the fiercely cold winters of north-eastern Siberia [1,2]. Climate
41 variability has indeed been a fundamental player shaping the specie’s adaptive structure in terms of
42 drought tolerance [3] or cold hardiness [4], among others. Although growth of Scots pine is essentially
43 limited by low temperatures in boreal forests [5–7], large areas in southern Siberia have scarce
44 precipitation and are therefore cold and dry. These transition forests (forest-steppe belt) represent the

45 ecotone between the boreal taiga to the north and the steppe grasslands to the south where
46 productivity is simultaneously limited by low temperatures (by severely confining the active
47 growing season) and water availability (by challenging tree performance during the short growing
48 period).

49 Global climate change is placing pressure on forest ecosystems from virtually all regions over
50 the globe [8–11]. In the case of Scots pine, growth can be promoted by increased temperatures at its
51 northern and upper distribution limits where productivity is primarily cold-limited [6,12]. In
52 contrast, decrease in productivity, reversal of carbon balance and even large-scale dieback episodes
53 have already been observed in the southern, drought-prone habitats of the species [13–15]. Moreover,
54 there is growing evidence that some temperature-limited sites may be progressively affected by
55 drought stress under warmer conditions due to exacerbated soil moisture deficit linked to increased
56 evapotranspirative demand [16–18]. Such opposing influences of low temperatures and drought on
57 growth dynamics bring much uncertainty about species vigour and productivity across the whole
58 distribution range [2,15] and, particularly, in cold–dry environments [19].

59 Tree rings are extensively used to assess climate change effects on forest ecosystems [20]. Most
60 dendroecological studies infer long-term changes in tree performance based on radial growth
61 patterns. However, additional information on leaf-level physiology can be gained through the
62 analysis of stable isotopes in tree rings [21]. On the one hand, carbon isotope discrimination ($\Delta^{13}\text{C}$)
63 depends on factors affecting CO_2 assimilation, as expressed in the ratio of photosynthetic rate to
64 stomatal conductance (A/g_s , or intrinsic water-use efficiency) [22]. On the other hand, oxygen isotope
65 composition ($\delta^{18}\text{O}$) is mainly influenced by source water isotopic composition (i.e., precipitation
66 modulated by residence time in soil and associated evaporation effects) and leaf water enrichment
67 due to transpiration at the stomata [23]. Both isotope types are therefore linked via effects at the leaf
68 level mediated through changes in stomatal conductance caused by varying soil moisture and
69 atmospheric evapotranspirative demand [24]. As $\delta^{18}\text{O}$ is not influenced by photosynthetic processes,
70 combining $\Delta^{13}\text{C}$ and $\delta^{18}\text{O}$ may allow separating stomatal and photosynthetic effects on tree
71 performance, which may eventually determine changes in productivity [25,26].

72 Despite pinewoods of the forest steppe zone of Central Siberia are receiving increasing attention
73 [27–30], the ecophysiological responses of Scots pine to current climate change remain poorly
74 investigated. Here, we assess climate effects on physiological processes underlying tree growth
75 patterns in two contrasting sites with regard to climate trends that are located near the moisture limit
76 of the species range at the southern edge of the boreal forest belt. This area offers an excellent
77 opportunity to test for global change impacts on forests growing under the combined effects of low
78 temperatures and water scarcity [31]. These interactions may expose trees to previously untested
79 bioclimatic envelopes, perhaps resulting in a relaxation of cold limitation modifying phenology and
80 an exacerbation of drought effects impacting on carbon and water budgets. In contrast to the large-
81 scale warming trend, local rainfall patterns in this region display significant spatial variability [32,33],
82 which may lead to a differential vulnerability of these stands to fluctuations in the moisture regime
83 during the short growing season. Based on these premises, the aim of this study was to understand
84 how *P. sylvestris* forests have responded to divergent climatic changes observed during the last 75
85 years in the region through the combined analysis of ring-width and stable isotopes. We
86 hypothesized that climatically-induced spatial variation in water availability determines the
87 ecophysiological responses and tree growth of Scots pine populations in cold–dry environments of
88 the Siberian forest-steppe ecotone and, ultimately, their responses to the ongoing temperature rise.
89 In particular, we assumed that WUE_i was uncoupled from changes in secondary growth in spite of
90 divergent climate trends at the site level (increasing warming-induced drought stress *vs.* enhanced
91 water availability and relaxation of cold limitation). Our specific objectives were (i) to examine how
92 climatic variability is reflected in tree-ring traits (ring-width, carbon and oxygen isotopes) of Scots
93 pine growing under a varying level of progressive exposition to drought stress; (ii) to evaluate trends
94 in tree growth (basal area increment, BAI) at stand level and how changes in productivity are
95 potentially linked with convergent physiological responses (i.e., increased WUE_i); and (iii) to
96 disentangle climate drivers controlling tree performance of these cold-dry forests and assess whether

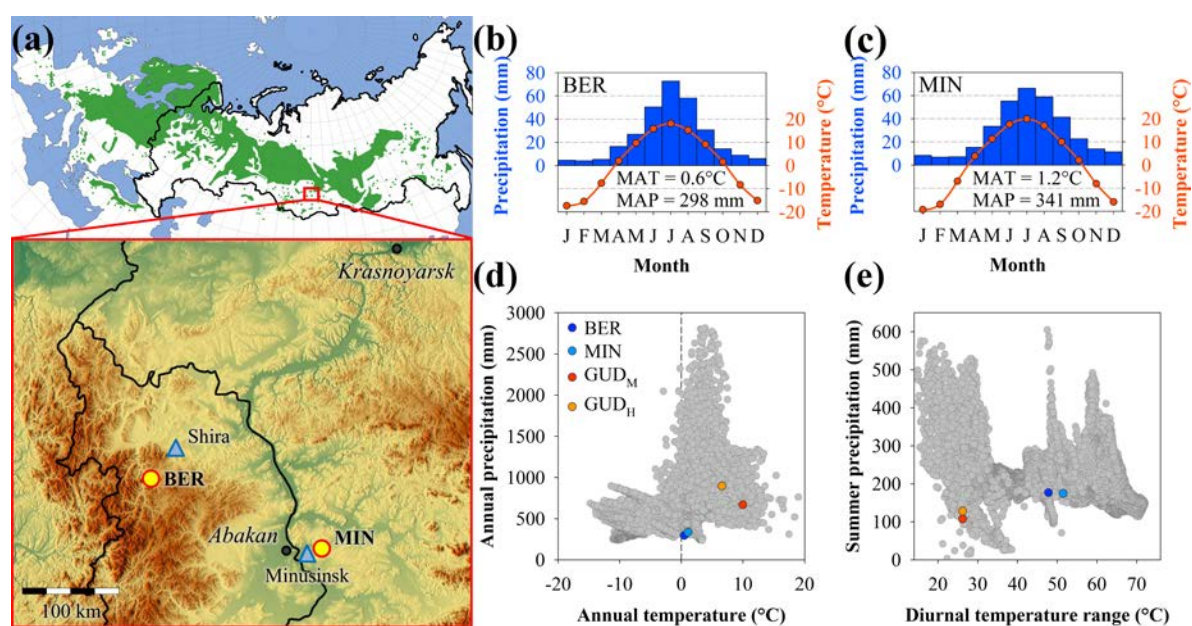
97 recent changes in local climate have modulated tree responses to drought stress during the growing
 98 period. To expand the scope of our inferences to other dry environments typical of warmer regions,
 99 we complemented our data with records compiled in a previous study [34] in which *P. sylvestris* was
 100 sampled in two stands of the eastern Iberian Peninsula.

101 2. Materials and Methods

102 2.1. Study sites

103 The study was conducted in two sites located 157 km apart in the northern edge of Altai–Sayan
 104 ecoregion in the south of Central Siberia (Russia). The region belongs to the forest-steppe belt which
 105 is bounded by the Siberian taiga in the north and the Mongolian grassland steppe in the south (Figure
 106 1a). The northern stand (Berenzhak site, BER; 54°16'N, 89°37'E) is formed on a gentle south-facing
 107 slope in the south-east of the Kuznetsk Alatau mountain range (615–621 m a.s.l.) (Table 1). The
 108 southern stand (Malaya Minusa site, MIN; 53°43'N, 91°50'E) is situated at the edge of a belt pine forest
 109 in the north of Minusinsk Depression (320–338 m a.s.l.) (Table 1). BER is an open mixed pine (*P.*
 110 *sylvestris*)–larch (*Larix sibirica*) forest with presence of scattered birch (*Betula pendula*) on a gray
 111 mountain soil, while MIN is an open monospecific pine forest with admixture of birch growing on a
 112 sandy soil with a humus layer of 8–10 cm. Both stands are characterized by an even age and size
 113 structure and have experienced minimal land use pressures (e.g., logging, grazing) over the twentieth
 114 century.

115
 116



117

118 **Figure 1.** Geographical location and climatic characteristic of the sampling sites in the forest steppe
 119 of Central Siberia. (a) *P. sylvestris* distribution (green shading; [35]) and location of the study area (top)
 120 and distribution of pine stands (bottom). Circles mark positions of the sampling sites and triangles
 121 denote Minusinsk and Shira meteorological stations used in the analyses. (b–c) Climate diagrams
 122 corresponding to northern (BER) and southern (MIN) sites. The primary *y*-axis indicates monthly
 123 precipitation (bars) and the secondary *y*-axis monthly mean temperature (lines). Average monthly
 124 values of climate factors were estimated based on the climate data from the nearest meteorological
 125 stations for the period 1940–2014. The mean annual temperature (MAT) and mean annual
 126 precipitation (MAP) are given for each site. (d–e) Autoecology diagram of *P. sylvestris* distribution
 127 with sites used in the analyses depicted as coloured circles: blue – BER (cold–dry site), light blue –
 128 MIN (cold–moist), red – GUD_M (warm–dry) and orange – GUD_H (warm–moist) (see section 2.6. for
 129 further details on GUD sites). The species range is derived from the EUFORGEN distribution map
 130 (<http://www.euforgen.org/species/pinus-sylvestris>).

131 **Table 1.** Geographic and dendrochronological characteristics of the sampling sites. Abbreviations:
 132 *EPS*, Expressed Population Signal; *Rbar*, mean inter-series correlation; *TRW*, tree-ring width; $\Delta^{13}\text{C}$,
 133 carbon isotope discrimination; $\delta^{18}\text{O}$, oxygen isotope composition. The mean values of tree-ring traits
 134 are estimated over the period 1940–2014 and the variability is expressed as standard deviation (\pm
 135 *SD*).

Site	Code	Latitude (N)	Longitude (E)	Altitude (m a.s.l.)	Nr trees ¹	Time span	<i>EPS</i> > 0.85	<i>Rbar</i> ²	<i>TRW</i> \pm <i>SD</i> (mm)	$\Delta^{13}\text{C}$ \pm <i>SD</i> (‰) ³	$\delta^{18}\text{O}$ \pm <i>SD</i> (‰) ³
Berenzhak	BER	54°15'41"	89°37'26"	615–621	20/19	1830–2014	1846	0.56	1.28 \pm 0.42	15.82 \pm 0.80	27.45 \pm 0.83
Malaya Minusa	MIN	53°43'25"	91°50'24"	320–338	20/17	1899–2014	1902	0.48	1.49 \pm 0.45	16.09 \pm 0.62	28.51 \pm 0.88

136 ¹ Number of trees (sampled/cross-dated)

137 ² Study period (1940–2014)

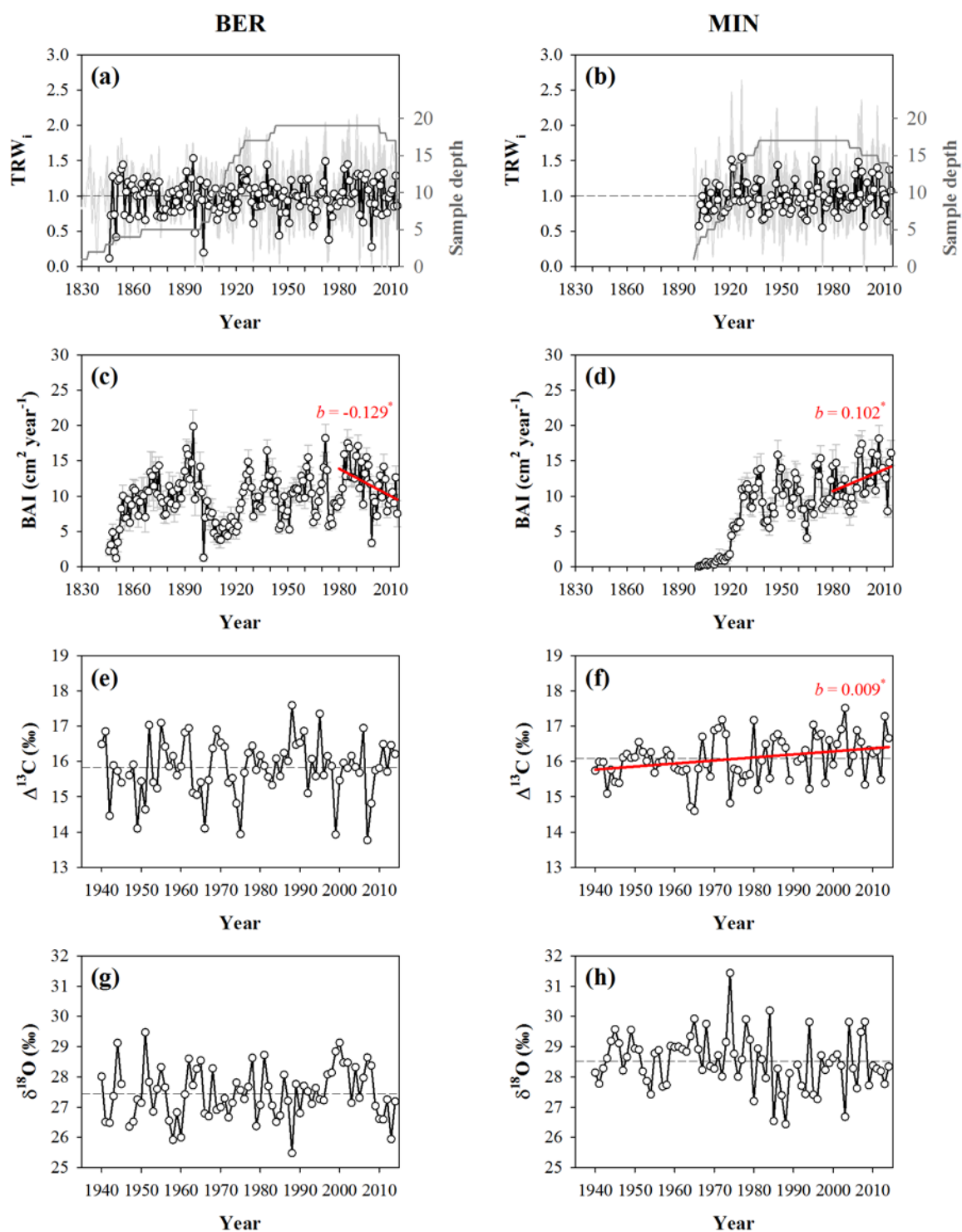
138 ³ For five trees used for isotope analysis

139
 140 The region is characterized by a moderately cold and dry continental climate with complex
 141 topography (mountain slopes, flats, depressions, etc.), which determines a wide diversity of local
 142 conditions. To characterize stand growing conditions, we obtained climate data from the nearest
 143 meteorological station to each study site, Shira (54°30'N, 89°56'E; 475 m a.s.l.) and Minusinsk
 144 (53°43'N, 91°42'E; 254 m a.s.l.) (Figure 1a), which are located at a distance of 33 km and 9 km from
 145 BER and MIN, respectively. According to the meteorological data, mean annual temperature is
 146 slightly higher in MIN (1.2°C) than in BER (0.6°C), with January being the coldest month (mean
 147 temperature = −19.3°C for MIN and −17.3°C for BER) and July the warmest month (+19.9°C for MIN
 148 and +18.0°C for BER) (period 1940–2014). The growing season starts at the end of April (MIN) or
 149 beginning of May (BER) and spans for 110–120 days on average (till end of August, approximately).
 150 Mean annual precipitation is lower in BER (298 mm) than in MIN (341 mm), with up to 70% occurring
 151 from May to August in both sites (Figure 1b,c). Although precipitation peaks during the growing
 152 period, potential evapotranspiration (PET) is over 2.5-fold greater than water supply during these
 153 months (PET = 502 mm for BER and 522 mm for MIN; [36]), hence resulting in recurrent summer
 154 droughts in the region.

155 2.2. Field sampling and tree-ring measurements

156 Field work was conducted at the end of August 2014. Twenty mature, dominant and healthy
 157 trees were randomly selected at each site and two cores from the same cross-slope side of the trunk
 158 were extracted at breast height with a 5-mm-diameter increment borer. Samples were oven-dried at
 159 60°C for 48 h and one core per tree was sanded with sandpapers of progressively finer grain until
 160 tree rings were clearly visible. The remaining core of every tree was kept intact for isotope analyses.
 161 Tree rings were visually cross-dated and measured with precision of 0.01 mm using a Lintab system
 162 (Rinntech, Heidelberg, Germany). Cross-dating was verified with the COFECHA program [37]. Poor
 163 samples failing to pass the cross-dating check were discarded for chronology developing (one ring-
 164 width series in BER and three in MIN).

165 In order to build indexed tree-ring width chronologies (*TRW_i*) for each site, the individual series
 166 were first standardized using a cubic-smoothing spline curve of 50 years with a 50%-frequency
 167 response cut-off. This procedure minimizes the effect of biological trends (e.g., tree age) and
 168 disturbances (e.g., stumps, fire scars) on radial growth, hence preserving high-frequency variability
 169 potentially related to climate. Standardization converted ring-width measurements into
 170 dimensionless indices with mean value of 1. Next, autoregressive models were applied to remove the
 171 first-order temporal autocorrelation in the detrended series and produce residual or pre-whitened
 172 indices. Finally, a biweight robust mean was computed to provide indexed chronologies for each site
 173 (Figure 2a,b). These procedures were done using the ARSTAN program [38]. The reliability of ring-



174

175 **Figure 2.** Tree-ring chronologies for BER (left panels) and MIN (right panels). (a, b) Residual tree-ring
 176 width indices (TRW_i) (grey lines) and master chronologies (black lines) for the period when Expressed
 177 Population Signal (EPS) exceeded 0.85 (see Table 1). The sampling size for each chronology is
 178 indicated by a dark grey line. (c, d) Mean basal area increment (BAI) calculated from the set of raw
 179 TRW series. Error bars denote standard errors. (e, f) Carbon isotope discrimination ($\Delta^{13}\text{C}$) and (g, h)
 180 oxygen isotope composition ($\delta^{18}\text{O}$) for the period 1940–2014. Dashed horizontal lines correspond to
 181 mean values of tree-ring traits (except BAI). Significant linear trends over time are depicted as red
 182 lines ($P < 0.05$), with the corresponding slope (b) of the trend indicated in each case.

183

184 width chronologies for capturing the hypothetical population signal was checked against the
 185 expressed population signal (*EPS*) criterion with a threshold value of 0.85 [39]. Inter-series correlation
 186 (*Rbar*) statistics and Principle Component Analysis (PCA) were used to estimate the internal
 187 coherence of each chronology [39]. These statistics were calculated over the period 1940–2014, when
 188 sample size was largest and growth had stabilized (i.e., excluding years of juvenile phase).

189 To characterize the absolute radial growth trends at each site, tree-ring width measurements
 190 were transformed to basal area increment (BAI). BAI represents an accurate indicator of tree vigour
 191 and growth over time because it accounts for the variation caused by adding volume to a circular
 192 stem [40]. On the other hand, it relies on the assumption of near-perfect circular and centred trunk
 193 sections, which was approximately met in both sites. BAI was calculated from the set of cross-dated
 194 tree-ring width series according to:

$$BAI = \pi(R_t^2 - R_{t-1}^2), \quad (1)$$

195 where *R* is the radius of the tree and *t* is the year of tree-ring formation. Finally, we calculated a mean
 196 BAI chronology for each site (Figure 2c,d). Trends in BAI were assessed independently for two
 197 consecutive periods (1940–1979 and 1980–2014) using linear regressions.

198 2.3. Stable isotope analyses

199 The five best cross-dated trees per site were selected for isotope measurements. Tree rings were
 200 split from the intact cores with annual resolution for the period 1940–2014. Rings corresponding to
 201 the same year and site were pooled into a single sample before analysis [41]. Every ten years (1944,
 202 1954, etc.), rings were analysed individually to estimate between-tree variability in the isotope
 203 signals. The resulting samples were homogenised with a ball mill (Retsch, Haan, Germany) and
 204 purified to α -cellulose following [42].

205 For the simultaneous determination of carbon and oxygen isotope ratios, about 1 mg of dry α -
 206 cellulose was weighed into silver foil capsules. Samples were converted to carbon monoxide via
 207 pyrolysis at 1080°C in a Costech elemental analyser and afterwards measured using a continuous
 208 flow Elementar Isoprime mass spectrometer. Isotope ratios were expressed as per mil deviations
 209 using the δ notation relative to Vienna Pee Dee Belemnite standard (for carbon) and Vienna Standard
 210 Mean Ocean Water (for oxygen) standards. The accuracy of the analyses (SD of working standards)
 211 was 0.12‰ ($\delta^{13}\text{C}$) and 0.26‰ ($\delta^{18}\text{O}$).

212 To account for changes in $\delta^{13}\text{C}$ of atmospheric CO_2 ($\delta^{13}\text{C}_{\text{air}}$), we calculated carbon isotope
 213 discrimination ($\Delta^{13}\text{C}$) from $\delta^{13}\text{C}_{\text{air}}$ and wood $\delta^{13}\text{C}$ ($\delta^{13}\text{C}$) (Figure 2e,f) following [22]:

$$\Delta^{13}\text{C} = \frac{\delta^{13}\text{C}_{\text{air}} - \delta^{13}\text{C}}{1 + \delta^{13}\text{C}}, \quad (2)$$

214 $\delta^{13}\text{C}_{\text{air}}$ applied to the samples varied between -8.36‰ and -6.86‰ (period 1940–2014) [43].

215 Indexed $\Delta^{13}\text{C}$ and $\delta^{18}\text{O}$ chronologies (hereafter $\Delta^{13}\text{C}_i$ and $\delta^{18}\text{O}_i$) were obtained following the same
 216 procedure used for TRW_i . Both indexed ring-width and isotope chronologies were used as input for
 217 climate analyses.

218 2.4. Intrinsic water-use efficiency

219 Using $\Delta^{13}\text{C}$ records, intrinsic water-use efficiency (WUE_i) was estimated according to:

$$\text{WUE}_i = \frac{C_a \times (b - \Delta^{13}\text{C})}{1.6 \times (b - a)}, \quad (3)$$

220 where C_a represents the atmospheric CO_2 concentration, a is the fractioning during diffusion through
 221 stomata ($\sim 4.4\text{‰}$) and b is the fractioning during carboxylation by Rubisco and PEP carboxylase
 222 ($\sim 27\text{‰}$) [22]. The factor 1.6 denotes the ratio of diffusivities of water vapour and CO_2 in the air. C_a
 223 values were taken from the National Oceanic and Atmospheric Administration (NOAA) Earth
 224 System Research Laboratory (<http://www.esrl.noaa.gov/>). We assumed near-constancy of differences

225 between stomatal and internal conductance over time as the high internal conductance of *P. sylvestris*
226 suggests low mesophyll limitations of photosynthesis [44].

227 In addition, theoretical WUE_i values were calculated according to three scenarios as proposed
228 by [45]. These scenarios describe how the C_i might follow the C_a increase over time: (i) either not at
229 all, when C_i is maintained constant; (ii) in a proportional way, when C_i/C_a is maintained constant; or
230 (iii) at the same rate, when $C_a - C_i$ is maintained constant. Initial C_i values were obtained for each site
231 by applying Eq. (3) to the average $\Delta^{13}C$ and C_a values of the first five years of the study period (1940–
232 1944). We used these scenarios to obtain theoretical WUE_i values that were compared to WUE_i
233 records obtained from measured $\Delta^{13}C$. To this end, the sum of squared differences between actual
234 and predicted WUE_i values was divided by the number of observations (years) for each scenario. The
235 square root of this quantity is the root mean square predictive difference (RMS_{PD}), for which smaller
236 values indicated more accurate theoretical predictions.

237 2.5. Climate analyses

238 Long-term series of monthly climate variables (temperature and precipitation) covered the
239 period 1940–2014 (with the exception of temperature data for BER, which were available since 1942).
240 In order to quantify drought severity, we estimated the Standardized Precipitation-
241 Evapotranspiration Index (SPEI; [46]) using the station climate data. A proxy of water deficit for the
242 growing season was also calculated as potential evapotranspiration exceeding precipitation ($PET - P$)
243 (P), which approximates the water budget on a monthly basis. PET was estimated following [36].

244 Monthly and seasonal (May–August) mean temperature, precipitation and the SPEI were used
245 to assess the relationships between tree-ring traits and climate for the period 1940–2014. Climate
246 series (temperature and precipitation) were standardised by fitting a cubic-smoothing spline curve
247 of 50 years with a 50%-frequency response cut-off. This was done to focus on the effect of high-
248 frequency local climate dynamics on tree performance rather than on the impact of long-term trends
249 (e.g., global warming). Instead, this impact was studied by examining tree responses to climate
250 independently for the two halves of the study period (1940–1979 and 1980–2014). The relationships
251 with climate were analysed through correlation and response functions from the previous October
252 to September of the year of tree-ring formation using the DendroClim2002 program [47]. The
253 significance of function parameters was estimated by drawing 1,000 bootstrapped samples with
254 replacement from the initial data set.

255 2.6. Comparative evaluation of Scots pine responses under cold–dry and warm–dry conditions

256 Our data were complemented with previously compiled records from dry environments typical
257 of warmer regions than the Siberian steppe in which *P. sylvestris* was sampled in two sites of the
258 Gúdar range (Iberian System, eastern Spain) along an altitudinal gradient: mid-altitude (GUD_M , 1615
259 m a.s.l.) and high-altitude (GUD_H , 2020 m a.s.l.) [34]. These *P. sylvestris* stands are subjected to
260 summer drought, but they differ in thermic regimes: climate is cold–dry in southern Siberia and
261 warm-dry in eastern Spain (Figure 1b,c). The difference in mean annual temperature between these
262 ecosystems is ca. 8°C, which translates into a more extended growing season in Spain (150 to 180 days
263 depending on altitude); on the other hand, total precipitation is about two-fold higher in Spain.
264 Altogether, the annual water deficit ($PET - P$) is about three-fold higher in the Gúdar sites than in
265 those of Central Siberia. Within each region, we distinguished between dry (BER, GUD_M) and
266 relatively wet (moist) conditions (MIN, GUD_H) during the growing season. In this way, we aimed at
267 quantifying the effects of growing conditions (atmospheric CO_2 concentration, climate) on WUE_i and
268 characterized the dependence of BAI on WUE_i changes over time across representative dry
269 environments of this species. The sampling protocol was similar across studies.

270 A set of mixed models testing the assumption of constant responses among stands to selected
271 covariates (i.e., heterogeneity of slopes ANOVA) was fitted to the data over the common period 1980–
272 2011. All variables were first checked for normality (Kolmogorov–Smirnov test) and logarithm-
273 transformed whenever necessary (i.e., BAI). First, we tested for the joint impact of atmospheric CO_2
274 (C_a) rise and climate (water deficit, WD) on WUE_i . To this end, WUE_i was modelled by introducing

275 the following terms in the model: Region (Siberia, Spain), Condition (dry, moist), the interaction
276 Region \times Condition, the covariate C_a and its interactions ($C_a \times$ Region, $C_a \times$ Condition and
277 $C_a \times$ Region \times Condition) and the covariate WD (PET – P for the period when mean temperature
278 exceeds 10°C; [48]) and its interactions (WD \times Region, WD \times Condition and
279 WD \times Region \times Condition). Alternative climatic variables such as temperature or precipitation were
280 not included in the final models because they were highly correlated with WD over the study period
281 ($r > 0.55$ for mean temperature; $r > 0.94$ for precipitation, $P < 0.001$ in all cases). WD was preferred
282 over temperature or precipitation because it can be interpreted as an integrative measure of drought
283 severity over the growing season in dry bioclimates [49,50]. The second model explained logarithm-
284 transformed BAI (logBAI) as a function of Region, Condition, the interaction Region \times Condition, the
285 covariate WUE_i and the interactions $WUE_i \times$ Region, $WUE_i \times$ Condition and
286 $WUE_i \times$ Region \times Condition. In all models, the tree identity was introduced as subject (random effect),
287 and year was introduced as repeated effect at the tree level with a first-order autoregressive
288 covariance structure to account for temporal autocorrelation. The significance of differences in tree
289 response (slopes) to the selected covariates was further examined by means of the following set of
290 orthogonal contrasts: (i) cold (Siberia) *vs.* warm (Spain) environments and (ii) dry (BER, GUD_M) *vs.*
291 moist (MIN, GUD_H) conditions. If second order interactions were significant, independent contrasts
292 for every site were evaluated. All analyses were performed with the MIXED procedure of SAS/STAT
293 software (ver. 9.4, SAS Inc., Cary, NC, USA) using restricted maximum likelihood (REML) for
294 estimation of model parameters. Relationships were considered significant at $P < 0.05$.

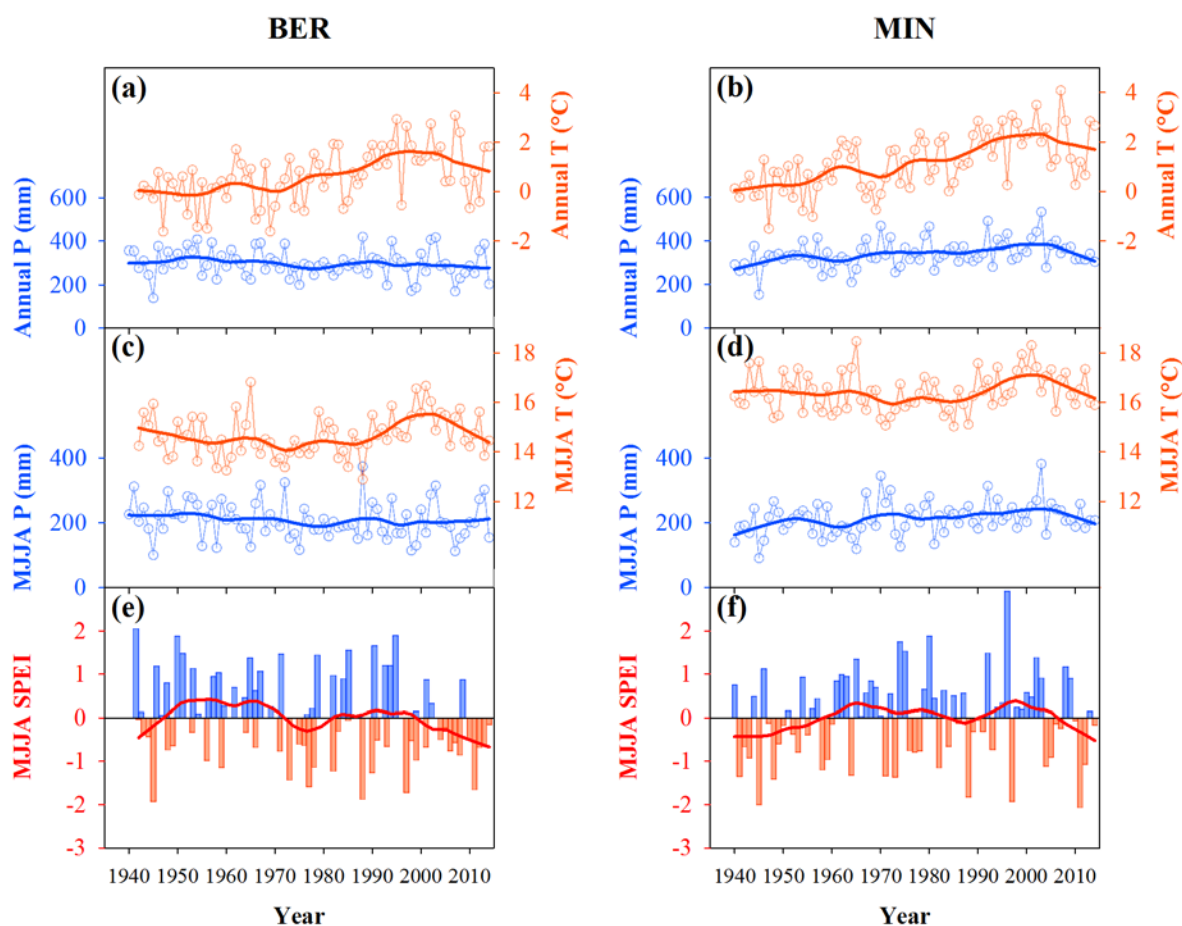
295 3. Results

296 3.1. Climate trends

297 Mean annual temperature increased at a similar rate of $\sim 0.03^\circ\text{C year}^{-1}$ in BER and MIN for the
298 period 1940–2014 (Figure 3a,b). There was also a steady increase in annual precipitation, but only in
299 MIN ($b = 0.93 \text{ mm year}^{-1}$) (Figure 3a,b). Changes in climate records during the growing season were
300 not consistent across sites. Particularly, mean May–August temperature significantly increased by
301 0.4°C from the first to the second half of the study period (1940–1979 and 1980–2014) in BER ($P < 0.05$;
302 two tailed Student's *t*-test), but remained approximately constant in MIN (Figure 3c,d). On the other
303 hand, May–August precipitation significantly increased by 22 mm during the latter period in MIN (P
304 < 0.05) (Figure 3c,d). Altogether, drier growing seasons became marginally more frequent after 1980
305 in BER according to May–August SPEI (Wilcoxon rank test, $P = 0.08$), suggesting an intensifying
306 impact of warming-induced drought stress which was especially noticeable at the turn of this century
307 (Figure 3e). On the other hand, no relevant changes in SPEI were observed in MIN (Figure 3f).

308 3.2. Characteristics of tree-ring chronologies

309 Tree-ring width chronologies having EPS over 0.85 spanned a period of 116 years in MIN and
310 185 years in BER (Table 1; Figure 2a,b). However, we restricted the study to the period of 1940 to 2014
311 in concord with the availability of climate data and also to avoid potential juvenile effects on tree
312 records. For this period, ring-width chronologies were characterized by a high inter-series correlation
313 (Table 1) and a high common variance captured by the first principal component (PC1 = 46.7% for
314 MIN and 59.0% for BER), which suggested that trees were responding to common external factors
315 (i.e., climate). Mean ring-width was higher in MIN ($1.49 \pm 0.45 \text{ mm}$; mean \pm SD) compared with BER
316 ($1.28 \pm 0.42 \text{ mm}$) (Table 1). Also there were consistently higher isotope values in MIN than in BER
317 ($16.09 \pm 0.62\text{‰}$ *vs.* $15.82 \pm 0.80\text{‰}$ for $\Delta^{13}\text{C}$; $28.51 \pm 0.88\text{‰}$ *vs.* $27.45 \pm 0.83\text{‰}$ for $\delta^{18}\text{O}$) (Table 1). In MIN,
318 $\Delta^{13}\text{C}$ values showed an increasing trend over time (Figure 2f), while no significant trend was found
319 for either $\Delta^{13}\text{C}$ in BER or $\delta^{18}\text{O}$ in both sites (Figure 2e,g,h).



320

321 **Figure 3.** Regional climate trends in BER (*left panels*) and MIN (*right panels*) for the period 1940–2014.
 322 (a, b) Annual (*upper panels*) and (c, d) growing season (May–August; *middle panels*) long-term changes
 323 in total precipitation (blue lines) and mean temperature (orange lines). The data were obtained from
 324 the nearest meteorological station to each sampling site (Shira station for BER; Minusinsk station for
 325 MIN). (e, f) Growing season (May–August) Standardized Precipitation-Evapotranspiration Index
 326 (MJJA SPEI). Positive values indicate wet years (blue bars), while negative values correspond to dry
 327 years (orange bars). Temporal trends in climate records (thick lines) are smoothed by LOESS fitting
 328 (span = 0.25). Significant (positive) linear trends over time were detected in mean annual temperature
 329 at both sites (BER: $b = 0.03^{\circ}\text{C year}^{-1}$, $P < 0.001$; MIN: $b = 0.03^{\circ}\text{C year}^{-1}$, $P < 0.001$) as well as in total
 330 annual precipitation at MIN ($b = 0.33 \text{ mm year}^{-1}$, $P < 0.01$).

331

332 **Table 2.** Pearson correlations involving indexed tree-ring traits (TRW_i , $\Delta^{13}\text{C}_i$ and $\delta^{18}\text{O}_i$) within and
 333 between sites for the period 1940–2014. Site codes are as in Table 1. *, $P < 0.05$; **, $P < 0.01$; ***, $P < 0.001$
 334 (non-significant correlation coefficients are indicated in italics).

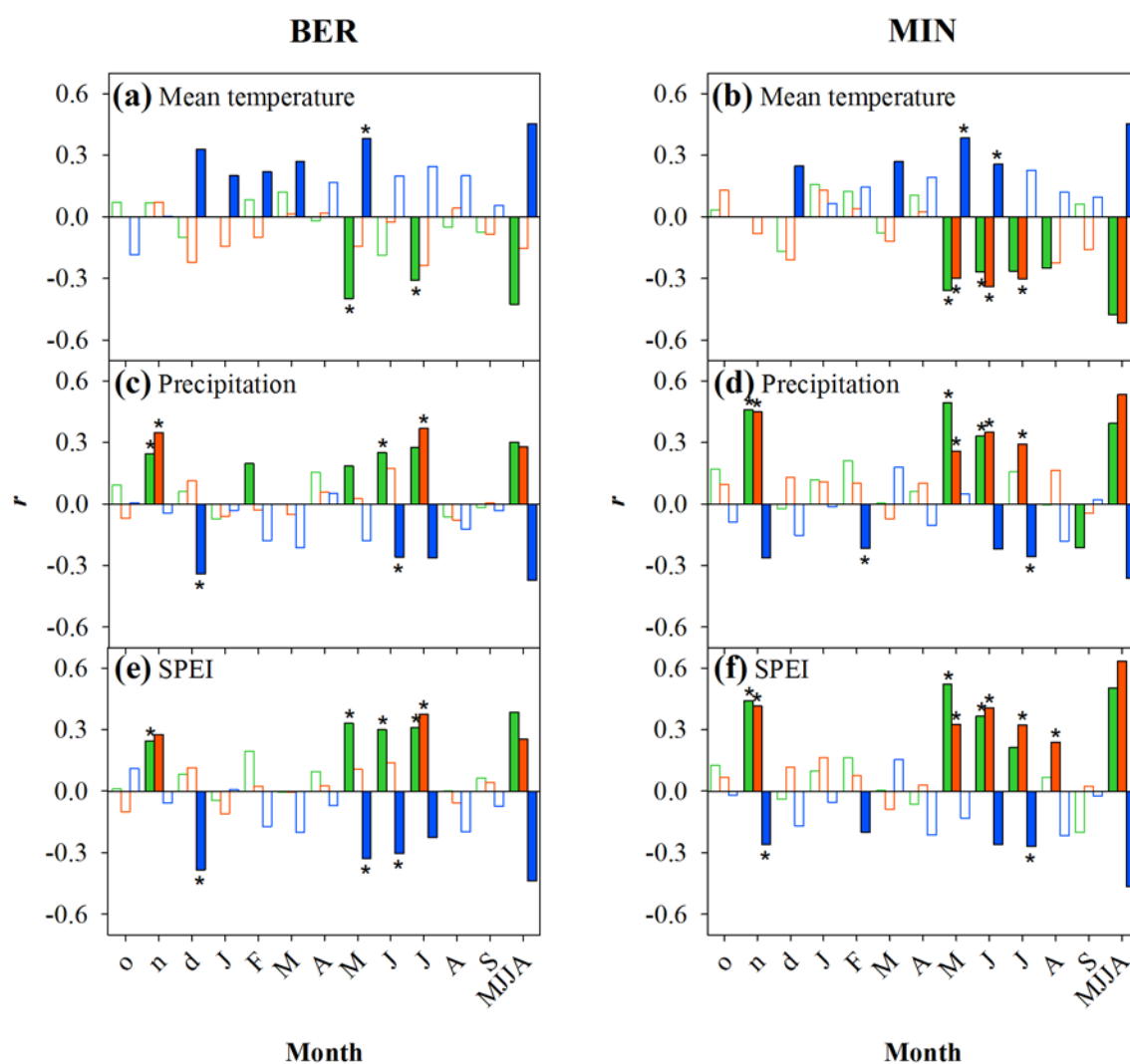
	BER – TRW _i	BER – $\Delta^{13}\text{C}_i$	BER – $\delta^{18}\text{O}_i$	MIN – TRW _i	MIN – $\Delta^{13}\text{C}_i$	MIN – $\delta^{18}\text{O}_i$
BER – TRW _i	—	0.51***	−0.25*	0.40***	0.46***	−0.51***
BER – $\Delta^{13}\text{C}_i$		—	−0.16	0.10	0.14	−0.31**
BER – $\delta^{18}\text{O}_i$			—	−0.29*	−0.29*	0.48***
MIN – TRW _i				—	0.63***	−0.25*
MIN – $\Delta^{13}\text{C}_i$					—	−0.60***
MIN – $\delta^{18}\text{O}_i$						—

335

336 Cross-correlations among indexed tree-ring parameters are shown in Table 2. There was a
 337 significant and positive relationship between TRW_i and $\Delta^{13}C_i$ at each site ($r = 0.51$ for BER and 0.63
 338 for MIN; $P < 0.001$), while a negative association was found between TRW_i and $\delta^{18}O_i$ ($r = -0.25$ for
 339 BER and -0.25 for MIN; $P < 0.05$). We also found a strong negative association between both isotopes
 340 in MIN ($r = -0.60$; $P < 0.001$). There was a good agreement between sites for TRW_i ($r = 0.40$; $P < 0.001$)
 341 and $\delta^{18}O_i$ ($r = 0.48$; $P < 0.001$), while the relationship was non-significant for $\Delta^{13}C_i$.

342 3.3. Relationships with climate

343 Growth responses to climate fluctuations were similar at both sites, although trees were overall
 344 more sensitive in MIN (Figure 4). TRW_i responded negatively to high May–August temperatures
 345 (Figure 4a,b) and was enhanced by previous November and current May–July precipitation (Figure
 346
 347



348

349 **Figure 4.** Tree responses to climate in BER (*left panels*) and MIN (*right panels*) for the period 1940–2014.
 350 The relationships with climate are based on bootstrapped correlations and response function partial
 351 regression coefficients between indexed tree-ring data corresponding to each site and (a, b) mean
 352 temperature, (c, d) precipitation, and (e, f) Standardized Precipitation-Evapotranspiration Index
 353 (SPEI). Climate signals are investigated at monthly- and seasonal- (May–August) time scales.
 354 Significant correlation and partial regression coefficients ($P < 0.05$) are indicated by filled bars and
 355 asterisks, respectively. Tree-ring traits are represented in green (TRW_i), orange ($\Delta^{13}C_i$), and blue
 356 ($\delta^{18}O_i$). Lowercase and uppercase letters in the x -axes correspond to months of the years before and
 357 during tree-ring formation, respectively.

358 4c,d). Such reactions resulted in positive growth responses to reduced drought stress (i.e., positive
 359 SPEI) during the growing season, particularly from May to July (Figure 4e,f). For $\Delta^{13}\text{C}$, there were
 360 positive correlations with July precipitation in BER and May–July precipitation in MIN. There was
 361 also a significant (positive) relationship with previous November precipitation in both sites (Figure
 362 4c,d). A strong negative response of $\Delta^{13}\text{C}$ to temperature during May–July was observed in MIN
 363 (Figure 4b). Overall, there were strong responses to drought (SPEI) in July in BER and May–August
 364 in MIN (Figure 4e,f). The correlations between $\delta^{18}\text{O}$ and temperature were positive, with the strongest
 365 responses found during May in BER and May–June in MIN, but also during previous winter–early
 366 spring (from previous December to March) at both sites (Figure 4a,b). Also $\delta^{18}\text{O}$ responded negatively
 367 to June–July precipitation in both sites, and to previous December precipitation in BER and previous
 368 November and current February precipitation in MIN (Figure 4c,d). Significant negative associations
 369 were found between $\delta^{18}\text{O}$ and SPEI in May–July (BER) and June–July (MIN) (Figure 4e,f).

370 Altogether the climate analysis showed that variability in tree growth and stable isotopes was
 371 sensitive to growing season (May–August) climate conditions, being most responsive to drought
 372 index (SPEI) as it integrates both temperature and precipitation signals. However, these relationships
 373 showed a recent shift in the case of stable isotopes (Figure S1 in supplementary material). This effect
 374 was especially noticeable in BER. Particularly, we found a significant positive correlation between
 375 $\Delta^{13}\text{C}$ and MJJA SPEI since the 1980s ($r = 0.55$, $P < 0.001$) which was lacking in the preceding period.
 376 Likewise, the relationship between $\delta^{18}\text{O}$ and SPEI strengthened recently ($r = -0.34$, $P < 0.05$ before
 377 1980; $r = -0.58$, $P < 0.001$ after 1980). In contrast, the dependence of tree-ring traits on SPEI during the
 378 growing season slightly weakened in MIN (Figure S1).

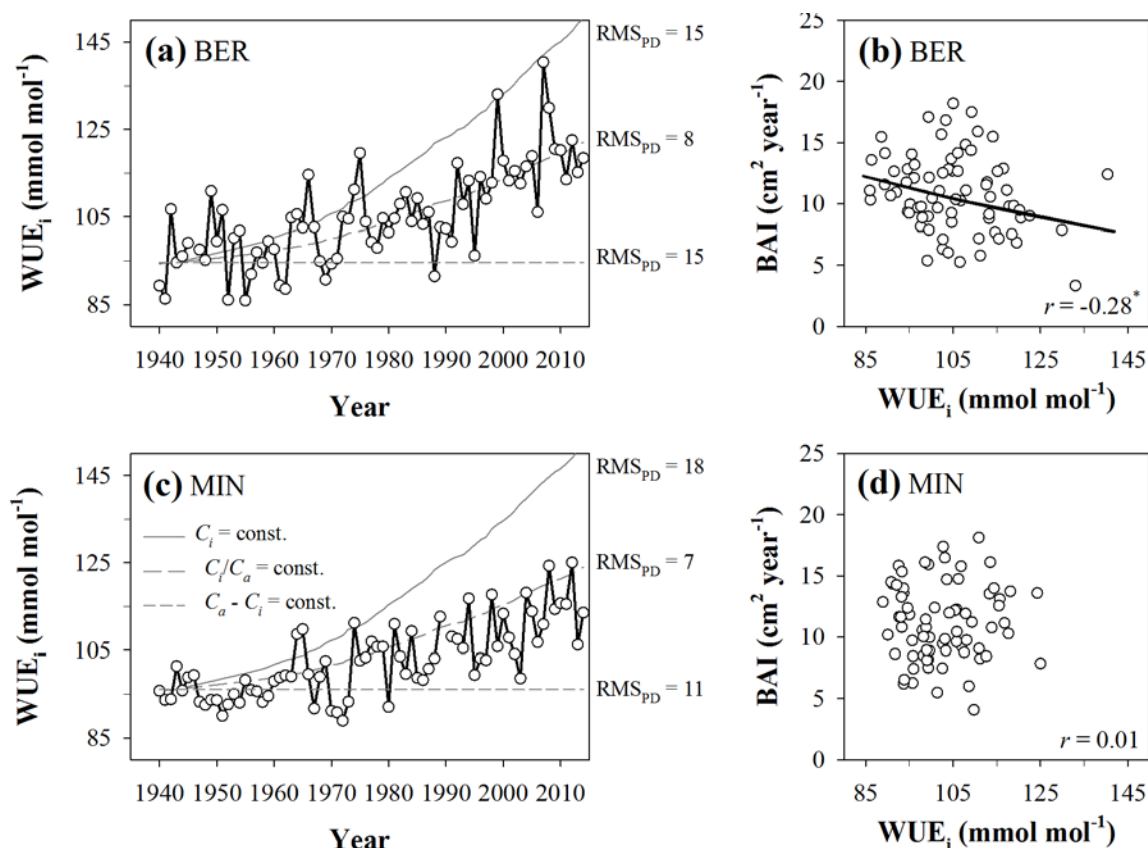
379 3.4. Temporal dynamics of WUE_i and relationships with BAI

380 The mean WUE_i across the period of 1940–2014 was significantly higher in BER (105.3 ± 11.08
 381 $\mu\text{mol mol}^{-1}$; mean \pm SD) than in MIN ($102.6 \pm 8.54 \mu\text{mol mol}^{-1}$) ($P < 0.01$). WUE_i showed increasing
 382 trends over time at both sites (Figure 5a,c), ranging from 20% (MIN) to 24% (BER) between the first
 383 (1940–1949) and the last decade (2005–2014) of the study period, with decadal increments of $2.9 \mu\text{mol}$
 384 mol^{-1} (MIN) and $3.6 \mu\text{mol mol}^{-1}$ (BER). The comparison of temporal trends of $\Delta^{13}\text{C}$ -based WUE_i
 385 records against three WUE_i scenarios ($C_i = \text{const.}$; $C_i/C_a = \text{const.}$; $C_a - C_i = \text{const.}$) indicated higher
 386 predictive power of the $C_i/C_a = \text{const.}$ scenario at both sites (Figure 5a,c).

387 The increasing WUE_i trend was accompanied by distinct growth patterns at the site level (Figure
 388 2c,d). Both sites showed a stable BAI from 1940 to 1979 with similar growth rates ($10.0 \pm 2.97 \text{ cm}^2$
 389 year^{-1} for BER; $9.9 \pm 2.88 \text{ cm}^2 \text{ year}^{-1}$ for MIN). After 1980, however, BAI showed a decreasing trend in
 390 BER ($b = -0.13 \text{ cm}^2 \text{ year}^{-2}$; $P < 0.05$), while it increased in MIN ($b = 0.10 \text{ cm}^2 \text{ year}^{-2}$; $P < 0.05$). Changes
 391 in long-term radial growth also affected site-level relationships with WUE_i (Figure 5b,d). For the
 392 initial period of 1940–1979, there were significantly negative correlations between BAI and WUE_i in
 393 BER ($r = -0.50$; $P < 0.01$) and MIN ($r = -0.54$; $P < 0.001$). However, while this association vanished after
 394 1980 in MIN ($r = -0.22$; $P = 0.22$), it strengthened in BER ($r = -0.56$; $P < 0.001$).

395 3.5. WUE_i and BAI trends in cold–dry (south Central Siberia) and warm–dry (eastern Spain) environments

396 WUE_i increased over time at a similar pace regardless of region and condition (Figure S2 in
 397 supplementary material). In particular, both C_a and WD significantly boosted WUE_i over the last three
 398 decades (Figure 6a,b; Table S1 in supplementary material). However, changes in WUE_i due to raising
 399 C_a were heterogeneous and depended simultaneously on condition (dry *vs.* moist) and region ($P <$
 400 0.001 for the term $C_a \times \text{Region} \times \text{Condition}$) (Table S1). The highest WUE_i increase to rising C_a was
 401 found under warm–moist conditions ($b = 0.456 \mu\text{mol mol}^{-1} \text{ ppm}^{-1}$), followed by cold–dry
 402 ($b = 0.340 \mu\text{mol mol}^{-1} \text{ ppm}^{-1}$), cold–moist ($b = 0.239 \mu\text{mol mol}^{-1} \text{ ppm}^{-1}$) and warm–dry conditions
 403 ($b = 0.149 \mu\text{mol mol}^{-1} \text{ ppm}^{-1}$) (Figure 6a). The contrast between warm–moist (GUD_H) and warm–dry
 404 (GUD_M) environments showed the most pronounced difference in the response of WUE_i to C_a
 405 ($P < 0.001$). On the other hand, there was no significant difference between cold–dry and cold–moist
 406 conditions (Figure 6a). In contrast, changes in WUE_i driven by water deficit (WD) were
 407 fundamentally due to differences between regions ($P < 0.01$ for the term $\text{WD} \times \text{Region}$) (Table S1).



408

409

410

411

412

413

414

415

416

417

Figure 5. Long-term evolution of intrinsic water-use efficiency (WUE_i) and its relationship with basal area increment (BAI) for BER (*upper panels*) and MIN (*lower panels*) for the period 1940–2014. **(a, c)** Temporal trends in intrinsic water-use efficiency (WUE_i) as related to three conceptual models assuming a constant intercellular CO_2 concentration ($C_i = \text{const.}$ scenario; solid line), a constant ratio between intercellular and atmospheric CO_2 concentrations ($C_i/C_a = \text{const.}$ scenario; long dashed line) and a constant difference between atmospheric and intercellular CO_2 concentrations ($C_a - C_i = \text{const.}$ scenario; short dashed line). The root mean square predictive difference (actual minus predicted values; RMS_{PD}) is shown for each model. **(b, d)** Relationships between WUE_i and basal area increment (BAI). A significant trend over time is depicted with a black line ($^*P < 0.05$).

418

419

420

421

422

423

424

425

426

Hence, WUE_i changes in response to WD were homogeneous within cold (Siberia) and within warm (Spain) environments, being larger (or more reactive to increasing WD) in trees growing in cold (Siberia) than in warm (Spain) conditions (difference = $0.042 \mu\text{mol mol}^{-1} \text{mm}^{-1}$; $P < 0.01$) (Figure 6b).

We also found an overall negative relationship between BAI and WUE_i (Figure 6c). However, the response of BAI to changes in WUE_i depended largely on growing condition ($P < 0.001$ for the term $WUE_i \times \text{Condition}$) (Table S2 in supplementary material). BAI decreased more strongly in response to enhanced WUE_i under dry than under moist conditions (difference = $-0.006 \text{cm}^2 \text{year}^{-1} \mu\text{mol}^{-1} \text{mol}$), regardless of region.

427

4. Discussion

428

429

430

431

432

433

434

435

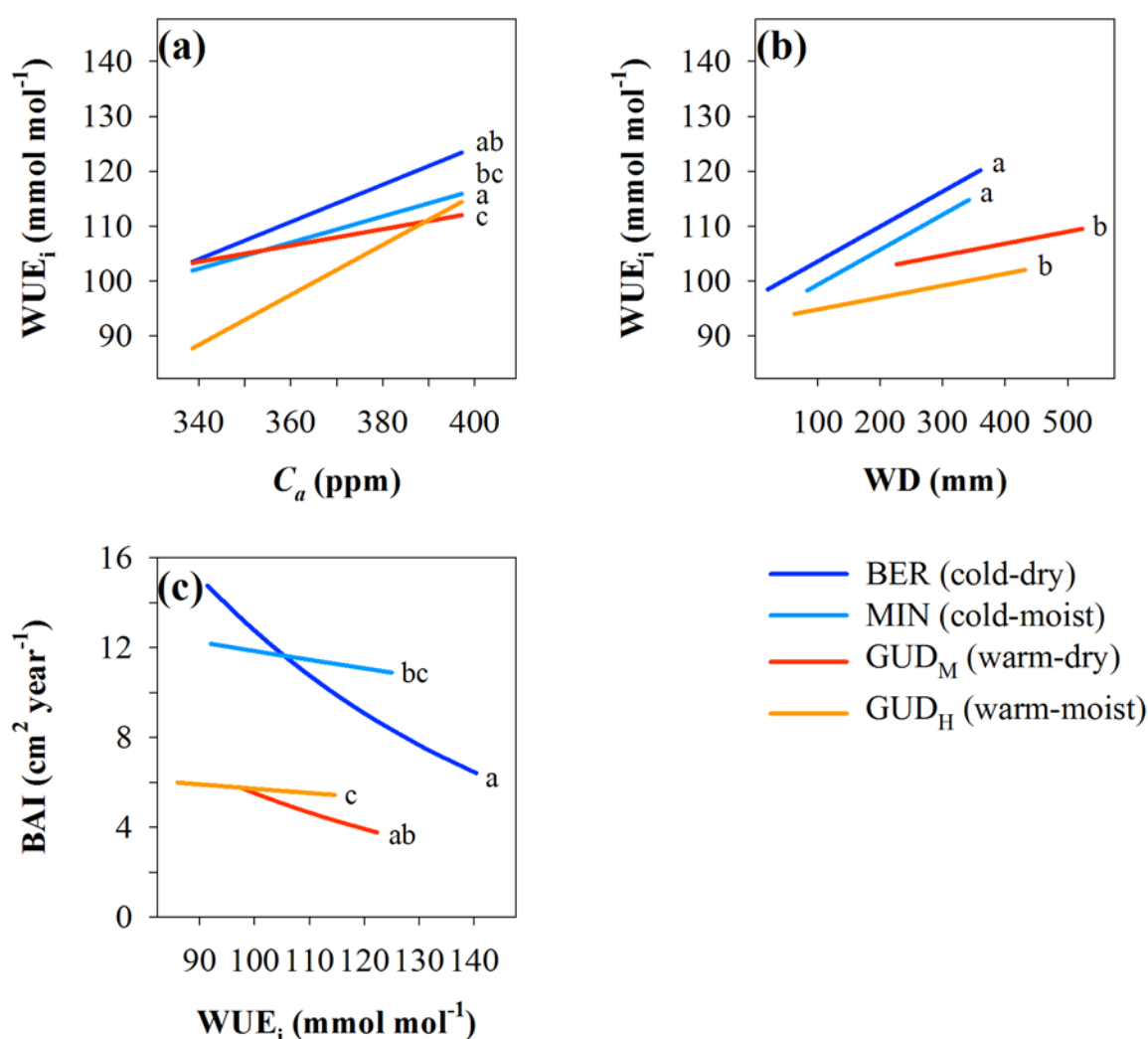
Scots pine growing in the dry steppes of Central Siberia is subjected to severe continentality (summer-winter temperature difference of *ca.* 40°C) and scarce annual precipitation (*ca.* 300 mm) concentrated in summer. The effects of such climate conditions on tree physiology, anatomy and reaction to climate warming have been fairly less explored [27,28,30] compared with other temperate and boreal regions where this widespread conifer is found. Despite a short and rainy growing season, the studied Scots pine stands showed a strong interannual dependence on water availability, which indicates that their performance in such cold-dry environments is limited by water shortage rather than by low temperatures. However, the impact of drought elicited contrasting site responses as

436 modulated by the joint effect of local climate and increasing atmospheric CO₂ concentrations over the
 437 last 75 years.

438 4.1. Site differences in tree performance as indicated by radial growth and stable isotopes

439 The good correspondence of ring-width variability between site chronologies, which was
 440 slightly lower than that found among series for each chronology, indicates that common factors
 441 determine Scots pine growth in the study region. Indeed, the observation that radial growth and $\Delta^{13}\text{C}$
 442 were tightly (positively) associated at both sites is expected under frequent and intense drought
 443 episodes, since both traits are strongly influenced by water shortage in Scots pine [34,51]. *P. sylvestris*
 444 is a conifer with a high stomatal sensitivity to water availability [52]. This isohydric behaviour has
 445 been supported by strong ¹³C discrimination in trees subjected to artificial irrigation [53] or sampled
 446 across water availability gradients [54,55].

447
 448



449

450 **Figure 6.** The effects of (a) atmospheric CO₂ concentration (C_a) and (b) growing season water deficit
 451 (WD; evapotranspirative demand exceeding precipitation) on intrinsic water-use efficiency (WUE_i)
 452 as a function of region (Central Siberia, Eastern Spain) and condition (dry, moist). (c) The effect of
 453 WUE_i on BAI as a function of region and condition. For each combination of region and condition,
 454 different letters indicate significant differences between slopes of responses according to a Student's
 455 *t* test ($\alpha = 0.05$).

456

457 Compared with MIN, pines in the drier but colder site (BER) showed lower radial growth and
458 $\Delta^{13}\text{C}$, hence pointing to a greater incidence of drought stress on tree physiology. Nevertheless, the
459 higher mean tree-ring $\delta^{18}\text{O}$ and the negative temporal association between $\Delta^{13}\text{C}$ and $\delta^{18}\text{O}$ in MIN
460 seem to contradict a higher water limitation occurring in BER. Both results could be understood as
461 the outcome of a higher evaporative enrichment of leaf water mediated by tighter stomatal control in
462 MIN (provided source water is roughly equivalent across sites) [24,56]. On the other hand, the
463 increase in annual and growing season precipitation in MIN is concomitant with the steady $\Delta^{13}\text{C}$
464 increase observed over the study period, whereas a significant relationship between $\Delta^{13}\text{C}$ and $\delta^{18}\text{O}$
465 found in BER after 1980 ($r = -0.33$, $P < 0.01$) suggests enhanced stomatal control of water losses under
466 increasing drought stress at this site. Altogether, we interpret these findings as an enhanced carbon
467 uptake in MIN with time, but a higher incidence of drought, hence reducing carbon assimilation, in
468 BER. Most likely, these patterns can be explained owing to the opposite trends observed in climate
469 factors during the growing season for the last 30 years (constant temperature and increasing
470 precipitation in MIN; increasing temperature and constant precipitation in BER).

471 4.2. Drought rather than low temperatures determines long-term regional performance of Scots pine

472 Scots pine growth was constrained by low precipitation and high temperatures during the short
473 growing season in the study area. The negative association of growth with warm spring-summer
474 temperatures across sites along with the positive effect of precipitation emphasize the relevance of
475 drought effects on pinewoods in the Siberian dry steppe [28,29]. Conversely, we did not find hints of
476 altered phenology nor of growth limitation by low temperatures during the growing season, as it is
477 the case in high altitude or high latitude Scots pine forests [6]. The higher sensitivity to climate found
478 in MIN was probably related to the low water retention and thermal inertia typical of sandy soils,
479 which made Scots pine more responsive to climatic fluctuations at this site. This may also explain the
480 higher stomatal sensitivity observed in MIN according to $\Delta^{13}\text{C}$ vs. $\delta^{18}\text{O}$ relationships. As suggested
481 by SPEI fluctuations, warmer temperatures led to enhanced evapotranspiration which, in
482 combination with low precipitation, hampered tree growth in such water-limited stands. On the
483 other hand, the positive influence of precipitation of previous November can be interpreted in terms
484 of snow cover depth, which protects roots from freeze damage in winter and serves as a source of
485 water early in the growing season [29].

486 The dependence of radial growth on growing season precipitation has been widely reported in
487 *P. sylvestris* and regarded as independent of temperature regime [27], which mainly determines the
488 length of the growing season. As most pines, *P. sylvestris* is an opportunistic species highly responsive
489 to precipitation pulses if water becomes limiting at any moment during growth [53,57]. The
490 prevalence of drought effects over low temperature restrictions on growth suggests that warming-
491 induced water limitation will progressively spread over areas of North Asia having low precipitation
492 but, also, very low temperatures (i.e., under extreme continentality), as already observed in Yakutia
493 [51]. Drought effects on Scots pine may not be limited to growth impairment, but they may also
494 hamper the formation of a functional xylem structure via a reduction of cell lumen and wall thickness,
495 as shown for the region [30,58].

496 The low correspondence between site chronologies for $\Delta^{13}\text{C}$ was unexpected since it is usually
497 assumed that carbon isotopes, as surrogates of the tree's carbon and water balance, are better tracers
498 of regional climate variability than ring-width [21,59]. In fact, $\Delta^{13}\text{C}$ and ring-width relationships with
499 climate were very similar in MIN (i.e., overlapping), whereas $\Delta^{13}\text{C}$ dependence on climate was
500 weaker in BER and concentrated in peak summer (July). Different conditions of moisture supply
501 between sites may have contributed to such differences, with pines in BER being buffered from short-
502 term changes in water availability due to higher soil water retention. Similarly to radial growth, a
503 strong precipitation signal of previous November was also recorded in $\Delta^{13}\text{C}$ at both sites, despite the
504 fact that the importance of November precipitation in the annual water budget is very limited (<5%
505 of total precipitation). This observation is puzzling and anticipates not only a mere protecting role of
506 the first snows to the root system, but also an important function in tree ecophysiology that would
507 deserve careful examination.

508 Relationships between $\delta^{18}\text{O}$ and climate pointed to a mixture of environmental signals. On the
509 one hand, negative associations with SPEI during the growing season suggest a leaf water enrichment
510 signal driven by air humidity that is passed on to the leaf organic matter and readily transferred to
511 the trunk, as supported by a high stomatal sensitivity and fast turnover rates in *P. sylvestris* [60]. On
512 the other hand, $\delta^{18}\text{O}$ relationships involving the snowfall season (especially with temperature)
513 indicate a strong signal of meteoric water that was registered in tree rings [61]. Both signal types were
514 quite consistent across sites but winter imprints in tree rings were stronger in BER, in agreement with
515 a higher soil water holding capacity which presumably made pines less dependent on climate
516 vagaries during the growing season.

517 The recent increase in tree sensitivity to growing season climate in BER confirms an amplifying
518 negative influence of summer drought on tree performance. This is in concord with a decreasing BAI
519 at this site; on the contrary, the effect of increasing precipitation in MIN seemed to overcome the
520 potentially negative effects of warming, boosting secondary growth (see next section). Indeed, *P.*
521 *syvestris* performance under varying water availability is essentially modulated by plastic responses
522 in functional characteristics such as WUE_i [57] or wood anatomy [62], among others.

523 4.3. Comparable WUE_i trends but contrasting BAI highlight the relevance of local conditions in forecasting 524 reactions to climate

525 CO_2 and climate are the main drivers of WUE_i variability in Scots pine [63]. An increasing trend
526 in WUE_i of ca. 22% across sites over the last 75 years, which is consistent with an scenario of constant
527 ratio of intercellular to ambient CO_2 concentration, agrees with the general performance of *P.*
528 *syvestris* across its distribution range (e.g., Alps mountains [64], central Europe [65] or north-eastern
529 China [66]) (but see [15]). This is in fact the most commonly observed response of forests worldwide
530 to increasing atmospheric CO_2 [45,65,67]. Although WUE_i showed such increasing regional trend,
531 BAI patterns started to drift apart in the 1980s (increasing in MIN, decreasing in BER), in concord
532 with the divergent climate trends observed in the study sites. In any case, BAI and WUE_i were either
533 unrelated (MIN) or negatively related (BER) over the whole study period and, in particular, during
534 the last 35 years. Many studies have also shown lack of CO_2 -driven growth stimulation in drought-
535 prone environments in spite of a recorded increase in WUE_i [68–72]. Instead, increasingly warmer
536 but wetter conditions probably boosted tree growth in MIN from 1980 onwards.

537 Our findings highlight how subtle changes in local conditions, mediated by CO_2 effects, may
538 differentially impact on radial growth in a transition area between the water-limited grasslands in
539 the south and the temperate mixed forests in the north of central Asia. Here, the particular site balance
540 between low temperature limiting the length of the growing season and scarce summer precipitation
541 limiting tree performance is turning into contrasting growth and physiological responses. This
542 observation was somewhat anticipated in a previous study based on provenance trials [73], in which
543 a reduction in tree height at age 13 of ca. -1% (or -4 cm, that is, almost no change) was forecasted in
544 the nearby site of Yermakovskiy (53°00'N, 94°00'E) between 1961–1990 and 2030. Scots pine in this
545 cold-dry region was predicted an intermediate reaction to future climate between that forecasted for
546 severely cold-limited, continental sites (with increments of up to +200% in Yakutsk, north-eastern
547 Eurasia) and that for warmer, less continental sites (with decrements of up to -39% in Volgograd,
548 south-eastern Europe) [73]. However, neither increasing atmospheric CO_2 effects nor nitrogen
549 deposition impacts on growth could be assessed in this study. While the relevance of CO_2 fertilization
550 in our results is discussed below, the incidence of N deposition on tree performance can be considered
551 negligible in the region [74].

552 4.4. Deciphering temporal dynamics in WUE_i and BAI across water-limited environments

553 The forest-steppe zone of Central Siberia and the sub-Mediterranean Gúdar mountain range of
554 eastern Spain represent climate extremes where *P. sylvestris* is subjected to recurrent summer
555 droughts (cf. Figure 1b,c). In both cases, the radial growth pattern of *P. sylvestris* [75] implies that
556 source (photosynthesis) and sink (xylogenesis) activities are jointly exposed to water shortage in
557 summer. Hence a relevant question arises about to what extent WUE_i and BAI are (un)coupled in

558 such contrasting thermal regimes. Both areas are subjected to low N deposition and, hence, the
559 observed increases in WUE_i were most likely unrelated to changes in nutrient availability.
560 Conversely, WUE_i trends were simultaneously dependent on atmospheric CO_2 (C_a) and water deficit
561 (WD), as reported elsewhere [63,64].

562 We found, however, that C_a and WD contributed differentially to changes in WUE_i depending
563 on region and level of water availability. Expressed in relative change over the last 75 years for a site-
564 constant WD, the highest and lowest WUE_i responses to C_a were observed in warm Mediterranean
565 environments (+27% and +7% under moist and dry conditions, respectively), with intermediate
566 values for the cold Siberian sites (+19% and +14% under moist and dry conditions, respectively). The
567 Mediterranean sites represent extreme and opposite reactions to C_a if compared with the mean WUE_i
568 increase due to CO_2 fertilization (ca. 22%) reported for conifers across Europe over the twentieth
569 century [76]. With high temperatures, the plasticity of WUE_i responses to C_a was strongly mediated
570 by water availability, in a way that a favourable moisture regime may allow increasing
571 photosynthesis over a long growing season and, hence, exploiting better a progressively larger C
572 substrate. This situation was also observed, but to a lesser extent, in cold Siberian sites having a
573 shorter growing period. Notably, the WUE_i dependence on water availability for a site-constant C_a
574 was stronger in Siberia than in Spain, with average WUE_i differences of 19% and 7% between WD
575 extremes, respectively (i.e. almost 3-fold higher sensitivity in Siberia). We hypothesize that the
576 shorter growing season in cold-dry environments may have prompted larger differences in gas
577 exchange of Scots pine among years compared with the more extended vegetative period typical of
578 warmer climates, which may allow plastic pines to deal more efficiently with seasonal fluctuations
579 in water availability.

580 Interestingly, BAI relationships with WUE_i followed site-specific patterns that differed from
581 those observed for WUE_i in its dependence on C_a and WD. The increase in WUE_i did not translate
582 into enhanced growth, but rather the opposite; in particular, BAI decreased more strongly at the
583 driest site of each region (−57% and −35% for Siberia and Spain, respectively) than at its wetter
584 counterparts (−10% and −9%, respectively). In dry areas, high WUE_i rates are associated with the cost
585 of reduced CO_2 assimilation in isohydric conifers such as Scots pine [77], which is beneficial for
586 protecting against xylem cavitation [78]. Our findings suggest a predictable pattern of radial growth
587 relationships with WUE_i that would be dependent on the difference in water deficit experienced
588 among stands for the prevailing thermic regime of a region. This assumption would require more
589 data gathered across the dry distribution edge of Scots pine.

590 5. Conclusions

591 The forest-steppe ecotone in Central Siberia is subjected to a delicate equilibrium posed by the
592 combined effects of current warming and drought on Scots pine, which results in contrasting site
593 performances in terms of growth and physiology. If water availability becomes progressively more
594 limiting, it may tip the balance towards strong reductions in growth rates despite the general
595 increasing trend in WUE_i . Conversely, pinewoods in the region could benefit from CO_2 fertilization
596 if an increase in temperature is accompanied by concomitant increments in precipitation, hence
597 boosting secondary growth. Altogether, our results highlight different fates of Scots pine forests in
598 cold-dry regions as mediated by concurrent changes in atmospheric CO_2 concentration and local
599 climate conditions.

600 **Supplementary Materials:** The following are available online at www.mdpi.com/link. Figure S1: Changes in
601 tree responses to seasonal drought stress (May–August Standardized Precipitation-Evapotranspiration Index)
602 over the two halves of the study period (1940–1979 and 1980–2014); Figure S2: Long-term evolution of intrinsic
603 water-use efficiency (WUE_i) of four Scots pine stands located in the forest-steppe zone of Central Siberia (cold
604 sites) and in sub-Mediterranean Eastern Spain (warm sites); Table S1: Significance of fixed effects of linear mixed
605 models with intrinsic water-use efficiency (WUE_i) explained as a function of Region, Condition, atmospheric
606 CO_2 concentration and growing season water deficit; Table S2: Significance of fixed effects of linear mixed
607 models with basal area increment (logBAI) explained as a function of Region, Condition and intrinsic water-use
608 efficiency.

609 **Acknowledgments:** This study was funded by the Spanish Government (grant number AGL2015-68274-C3-3-
610 R) and the Russian Science Foundation (project numbers 14-14-00295, sampling and tree-ring data obtainment
611 and 14-14-00219-P, mathematical approach). We acknowledge P. Sopena and M.J. Pau for technical assistance.

612 **Author Contributions:** A.V.K., J.V. and M.S. conceived and designed the experiment; A.V.K. was responsible
613 for field data collection, tree-ring cross-dating and measurements; M.S. and R.T.W.S. performed isotope analysis;
614 T.A.S. carried out the analyses and led the writing, with substantial contributions from J.V., A.V.K., M.S. and
615 R.T.W.S. All the authors read and approved the final draft of the manuscript.

616 **Conflicts of Interest:** The authors declare no conflict of interest.

617 References

- 618 1. Carlisle, A.; Brown, A.H.F. *Pinus sylvestris* L. *J. Ecol.* **1968**, *56*, 269–307, DOI: 10.2307/2258078.
- 619 2. Matías, L.; Jump, A.S. Interactions between growth, demography and biotic interactions in determining
620 species range limits in a warming world: the case of *Pinus sylvestris*. *For. Ecol. Manag.* **2012**, *282*, 10–22, DOI:
621 10.1016/j.foreco.2012.06.053.
- 622 3. Taeger, S.; Fussi, B.; Konnert, M.; Menzel, A. Large-scale genetic structure and drought-induced effects on
623 European Scots pine (*Pinus sylvestris* L.) seedlings. *Eur. J. For. Res.* **2013**, *132*, 481–496, DOI: 10.1007/s10342-
624 013-0689-y.
- 625 4. Gyertich, M. Provenance variation in growth and phenology. In *Genetics of Scots Pine*; Gyertich, M., Mátyás,
626 C., Eds.; Elsevier: Amsterdam, The Netherlands, 1991; pp. 87–101, ISBN: 9781483291635.
- 627 5. Gervais, B.R.; MacDonald, G.M. A 403-year record of July temperatures and treeline dynamics of *Pinus*
628 *syvestris* from the Kola Peninsula, northwest Russia. *Arct. Antarct. Alp. Res.* **2000**, *32*, 295–302, DOI:
629 10.2307/1552528.
- 630 6. Briffa, K.R.; Shshov, V.V.; Melvin, T.M.; Vaganov, E.A.; Grudd, H.; Hantemirov, R.M.; Eronen, M.;
631 Naurzbaev, M.M. Trends in recent temperature and radial tree growth spanning 2000 years across
632 northwest Eurasia. *Phil. Trans. R. Soc. B.* **2008**, *363*, 2271–2284, DOI: 10.1098/RSTB.2007.2199.
- 633 7. McCarroll, D.; Loader, N.J.; Jalkanen, R.; Gagen, M.H.; Grudd, H.; Gunnarson, B.E.; Kirchhefer, A.J.;
634 Friedrich, M.; Linderholm, H.W.; Lindholm, M.; Boettger, T.; Los, S.O.; Remmele, S.; Kononov, Y.M.;
635 Yamazaki, Y.H.; Young, G.H.F.; Zorita, E. A 1200-year multiproxy record of tree growth and summer
636 temperature at the northern pine forest limit of Europe. *The Holocene* **2013**, *23*, 471–484, DOI:
637 10.1177/0959683612467483.
- 638 8. Bonan, G.B. Forests and climate change: forcings, feedbacks, and the climate benefits of forests. *Science* **2008**,
639 *320*, 1444–1449, DOI: 10.1126/science.1155121.
- 640 9. Choat, B.; Jansen, S.; Brodribb, T.J.; Cochard, H.; Delzon, S.; Bhaskar, R.; Bucci, S.J.; Feild, T.S.; Gleason,
641 S.M.; Hacke, U.G.; Jacobsen, A.L.; Lens, F.; Maherali, H.; Martínez-Vilalta, J.; Mayr, S.; Mencuccini, M.;
642 Mitchell, P.J.; Nardini, A.; Pittermann, J.; Pratt, R.B.; Sperry, J.S.; Westoby, M.; Wright, I.J.; Zanne, A.E.
643 Global convergence in the vulnerability of forests to drought. *Nature* **2012**, *491*, 752–755, DOI:
644 10.1038/nature11688.
- 645 10. Williams, A.P.; Allen, C.D.; Macalady, A.K.; Griffin, D.; Woodhouse, C.A.; Meko, D.M.; Swetnam, T.W.;
646 Rauscher, S.A.; Seager, R.; Grissino-Mayer, H.D.; Dean, J.S.; Cook, E.R.; Gangodagamage, C.; Cai, M.;
647 McDowell, N.G. Temperature as a potent driver of regional forest drought stress and tree mortality. *Nat.*
648 *Clim. Chang.* **2013**, *3*, 292–297, DOI: 10.1038/nclimate1693.
- 649 11. Allen, C.D.; Breshears, D.D.; McDowell, N.G. On underestimation of global vulnerability to tree mortality
650 and forest die-off from hotter drought in the Anthropocene. *Ecosphere* **2015**, *6*, 129, DOI: 10.1890/ES15-
651 00203.1.
- 652 12. Kullman, L.; Kjällgren, L. Holocene pine tree-line evolution in the Swedish Scandes: Recent tree-line rise
653 and climate change in a long-term perspective. *Boreas* **2006**, *35*, 159–168, DOI: 10.1080/03009480500359137.
- 654 13. Martínez-Vilalta, J.; Piñol, J. Drought-induced mortality and hydraulic architecture in pine populations of
655 the NE Iberian Peninsula. *For. Ecol. Manag.* **2002**, *161*, 247–256, DOI: 10.1016/S0378-1127(01)00495-9.
- 656 14. Rigling, A.; Bigler, C.; Eilmann, B.; Feldmeyer-Christe, E.; Gimmi, U.; Ginzler, C.; Graf, U.; Mayer, P.;
657 Vacchiano, G.; Weber, P.; Wohlgemuth, T.; Zweifel, R.; Dobbertin, M. Driving factors of a vegetation shift
658 from Scots pine to pubescent oak in dry Alpine forests. *Glob. Chang. Biol.* **2013**, *19*, 229–240, DOI:
659 10.1111/gcb.12038.

- 660 15. Hereş, A.M.; Voltas, J.; Claramunt López, B.; Martínez-Vilalta, J. Drought-induced mortality selectively
661 affects Scots pine trees that show limited intrinsic water-use efficiency responsiveness to raising
662 atmospheric CO₂. *Funct. Plant Biol.* **2014**, *41*, 244–256. DOI: 10.1071/FP13067.
- 663 16. Lloyd, A.H.; Bunn, A.G. Responses of the circumpolar boreal forest to 20th century climate variability.
664 *Environ. Res. Lett.* **2007**, *2*, 045013, DOI: 10.1088/1748-9326/2/4/045013.
- 665 17. Buermann, W.; Parida, B.R.; Jung, M.; MacDonald, G.M.; Tucker, C.J.; Reichstein, M. Recent shift in
666 Eurasian boreal forest greening response may be associated with warmer and drier summers. *Geophys. Res.*
667 *Lett.* **2014**, *41*, 1995–2002, DOI: 10.1002/2014GL059450.
- 668 18. Dũthorn, E.; Schneider, L.; Günther, B.; Gläser, S.; Esper, J. Ecological and climatological signals in tree-
669 ring width and density chronologies along a latitudinal boreal transect. *Scand. J. For. Res.* **2016**, *31*, 750–757,
670 DOI: 10.1080/02827581.2016.1181201.
- 671 19. Sánchez-Salguero, R.; Camarero, J.J.; Hevia, A.; Madrigal-González, J.; Linares, J. C.; Ballesteros-Canovas,
672 J. A.; Sánchez-Miranda, A.; Alfaro-Sánchez, R. What drives growth of Scots pine in continental
673 Mediterranean climates: drought, low temperatures or both? *Agric. For. Meteorol.* **2015**, *206*, 151–162, DOI:
674 10.1016/j.agrformet.2015.03.004.
- 675 20. Babst, F.; Poulter, B.; Bodesheim, P.; Mahecha, M.D.; Frank, D.C. Improved tree-ring archives will support
676 earth-system science. *Nat. Ecol. Evol.* **2017**, *1*, 0008, DOI: 10.1038/s41559-016-0008.
- 677 21. McCarroll, D.; Loader, N.J. Stable isotopes in tree rings. *Quat. Sci. Rev.* **2004**, *23*, 771–801, DOI:
678 10.1016/j.quascirev.2003.06.017.
- 679 22. Farquhar, G.D.; Ehleringer, J.; Hubick, K. Carbon isotope discrimination and photosynthesis. *Annu. Rev.*
680 *Plant Physiol. Plant Mol. Biol.* **1989**, *40*, 503–537, DOI: 10.1146/annurev.pp.40.060189.002443.
- 681 23. Yakir, D. Variations in the natural abundances of oxygen-18 and deuterium in plant carbohydrates. *Plant*
682 *Cell Environ.* **1992**, *15*, 1005–1020, DOI: 10.1111/j.1365-3040.1992.tb01652.x.
- 683 24. Scheidegger, Y.; Saurer, M.; Bahn, M.; Siegwolf, R.T.W. Linking stable oxygen and carbon isotopes with
684 stomatal conductance and photosynthetic capacity: a conceptual model. *Oecologia* **2000**, *125*, 350–357, DOI:
685 10.1007/s004420000466.
- 686 25. Barbour, M.M.; Walcroft, A.S.; Farquhar, G.D. Seasonal variation in δ¹³C and δ¹⁸O of cellulose from growth
687 rings of *Pinus radiata*. *Plant Cell Environ.* **2002**, *25*, 1483–1499, DOI: 10.1046/j.0016-8025.2002.00931.x.
- 688 26. Barnard, H.R.; Brooks, J.R.; Bond, B.J. Applying the dual-isotope conceptual model to interpret
689 physiological trends under controlled conditions. *Tree Physiol.* **2012**, *32*, 1183–1198, DOI:
690 10.1093/treephys/tps078.
- 691 27. Rigling, A.; Waldner, P.O.; Forster, T.; Bräker, O.U.; Pouttu, A. Ecological interpretation of tree-ring width
692 and intraannual density fluctuations in *Pinus sylvestris* on dry sites in the central Alps and Siberia. *Can. J.*
693 *For. Res.* **2001**, *31*, 18–31. DOI: 10.1139/cjfr-31-1-18.
- 694 28. Wu, X.; Liu, H.; Guo, D.; Anenkhonov, O.A.; Badmaeva, N.K.; Sandanov D.V. Growth decline linked to
695 warming-induced water limitation in hemi-boreal forests. *PLoS One* **2012**, *8*, e42619, DOI:
696 10.1371/journal.pone.0042619.
- 697 29. Babushkina, E.A.; Vaganov, E.A.; Belokopytova, L.V.; Shishov, V.V.; Grachev, A.M. Competitive strength
698 effect in the climate response of Scots pine radial growth in south-Central Siberia forest-steppe. *Tree Ring*
699 *Res.* **2015**, *71*, 106–117, DOI: 10.3959/1536-1098-71.2.106.
- 700 30. Fonti, P.; Babushkina, E.A. Tracheid anatomical responses to climate in a forest-steppe in Southern Siberia.
701 *Dendrochronologia* **2016**, *39*, 32–41, DOI: 10.1016/j.dendro.2015.09.002.
- 702 31. Knorre, A.A.; Siegwolf, R.T.W.; Saurer, M.; Sidorova, O.V.; Vaganov, E.A.; Kirilyanov, A.V. Twentieth
703 century trends in tree ring stable isotopes (δ¹³C and δ¹⁸O) of *Larix sibirica* under dry conditions in the forest
704 steppe in Siberia. *J. Geophys. Res.* **2010**, *115*, G03002, DOI 10.1029/2009JG000930.
- 705 32. Soja, A.J.; Tchebakova, N.M.; French, N.H.F.; Flannigan, M.D.; Shugart, H.H.; Stocks, B.J.; Sukhinin, A.I.;
706 Parfenova, E.I.; Chapin III, F.S.; Stackhouse Jr.; P.W. Climate-induced boreal forest change: predictions
707 versus current observations. *Glob. Planet. Change* **2007**, *56*, 274–296, DOI: 10.1016/j.gloplacha.2006.07.028.
- 708 33. Tchebakova, N.M.; Parfenova, E.I.; Soja, A.J. Climate change and climate-induced hot spots in forest shifts
709 in central Siberia from observed data. *Reg. Environ. Change* **2011**, *11*, 817–827, DOI: 10.1007/s10113-011-0210-
710 4.
- 711 34. Shestakova, T.A.; Camarero, J.J.; Ferrio, J.P.; Knorre, A.A.; Gutiérrez, E.; Voltas, J. Increasing drought effects
712 on five European pines modulate Δ¹³C-growth coupling along a Mediterranean altitudinal gradient. *Funct.*
713 *Ecol.* **2017**, *31*, 1359–1370, DOI: 10.1111/1365-2435.12857.

- 714 35. Critchfield, W.B.; Little Jr., E.L. *Geographic distribution of the pines of the world*. U.S. Dept. of Agriculture,
715 Forest Service: Washington, D.C., USA, 1966, 97 pp., DOI: 10.5962/bhl.title.66393.
- 716 36. Hargreaves, G.H.; Samani, Z.A. Estimating potential evapotranspiration. *J. Irrig. Drain. Div.* **1982**, *108*, 225–
717 230.
- 718 37. Holmes, R.L. Computer-assisted quality control in tree-ring dating and measurement. *Tree-Ring Bull.* **1983**,
719 *43*, 69–78.
- 720 38. Cook, E.R.; Krusic, P.J. *Program ARSTAN: A tree-ring standardization program based on detrending and*
721 *autoregressive time series modeling, with interactive graphics*; Columbia University: Palisades, NY, USA, 2005,
722 14 pp.
- 723 39. Wigley, T.M.L.; Briffa, K.R.; Jones, P.D. On the average of correlated time series, with applications in
724 dendroclimatology and hydrometeorology. *J. Clim. Appl. Meteorol.* **1984**, *23*, 201–213, DOI: 10.1175/1520-
725 0450(1984)023<0201:OTAVOC>2.0.CO;2.
- 726 40. Biondi, F.; Qeadan, F. A theory-driven approach to tree-ring standardization: defining the biological trend
727 from expected basal area increment. *Tree-Ring Res.* **2008**, *64*, 81–96, DOI: 10.3959/2008-6.1.
- 728 41. Leavitt, S.W. Tree-ring isotopic pooling without regard to mass: no difference from averaging $\delta^{13}\text{C}$ values
729 of each tree. *Chem. Geol.* **2008**, *252*, 52–55, DOI: 10.1016/j.chemgeo.2008.01.014.
- 730 42. Ferrio, J.P.; Voltas, J. Carbon and oxygen isotope ratios in wood constituents of *Pinus halepensis* as indicators
731 of precipitation, temperature and vapor pressure deficit. *Tellus B – Chem. Phys. Meteorol.* **2005**, *57*, 164–173,
732 DOI: 10.1111/j.1600-0889.2005.00137.x.
- 733 43. Ferrio, J.P.; Araus, J.L.; Buxó, R.; Voltas, J.; Bort, J. Water management practices and climate in ancient
734 agriculture: inferences from the stable isotope composition of archaeobotanical remains. *Veget. Hist.*
735 *Archaeobot.* **2005**, *14*, 510–517, DOI: 10.1007/s00334-005-0062-2.
- 736 44. Veromann-Jürgenson, L.L.; Tosens, T.; Laanisto, L.; Niinemets, Ü. Extremely thick cell walls and low
737 mesophyll conductance: welcome to the world of ancient living! *J. Exp. Bot.* **2017**, *68*, 1639–1653, DOI:
738 10.1093/jxb/erx045.
- 739 45. Saurer, M.; Siegwolf, R.; Schweingruber, F. Carbon isotope discrimination indicates improving water-use
740 efficiency of trees in northern Eurasia over the last 100 years. *Glob. Chang. Biol.* **2004**, *10*, 2109–2120, DOI:
741 10.1111/j.1365-2486.2004.00869.x.
- 742 46. Vicente-Serrano, S.M.; Beguería, S.; López-Moreno, J.I. A multi-scalar drought index sensitive to global
743 warming: The Standardized Precipitation Evapotranspiration Index. *J. Clim.* **2010**, *23*, 1696–1718, DOI:
744 10.1175/2009JCLI2909.1.
- 745 47. Biondi, F.; Waikul, K. DENDROCLIM 2002: A C++ program for statistical calibration of climate signals in
746 tree-ring chronologies. *Comput. Geosci.* **2004**, *30*, 303–311, DOI: 10.1016/j.cageo.2003.11.004.
- 747 48. Swidrak, I.; Gruber, A.; Kofler, W.; Oberhuber, W. Effects of environmental conditions on onset of xylem
748 growth in *Pinus sylvestris* under drought. *Tree Physiol.* **2011**, *31*, 483–493, DOI: 10.1093/treephys/tpr034.
- 749 49. UNESCO. *Map of the world distribution of arid regions: Explanatory note*; UNESCO: Paris, France, 1979, p. 54;
750 ISBN: 9789231014840.
- 751 50. Le Houerou, H.N. An agro-bioclimatic classification of arid and semiarid lands in the isoclimatic
752 Mediterranean zones. *Arid Land Res. Manag.* **2004**, *18*, 301–346, DOI: 10.1080/15324980490497302.
- 753 51. Kagawa, A.; Naito, D.; Sugimoto, A.; Maximov, T.C. Effects of spatial variability in soil moisture on widths
754 and $\delta^{13}\text{C}$ values of eastern Siberian tree rings, *J. Geophys. Res.* **2003**, *108*, 4500, DOI: 10.1029/2002JD003019.
- 755 52. Irvine, J., Perks, M.P., Magnani, F., Grace, J. The response of *Pinus sylvestris* to drought: stomatal control of
756 transpiration and hydraulic conductance. *Tree Physiol.* **1998**, *18*, 393–402, DOI: 10.1093/treephys/18.6.393.
- 757 53. Eilmann, B.; Buchmann, N.; Siegwolf, R.; Saurer, M.; Cherubini, P.; Rigling, A. Fast response of Scots pine
758 to improved water availability reflected in tree-ring width and $\delta^{13}\text{C}$. *Plant Cell Environ.* **2010**, *33*, 1351–1360,
759 DOI: 10.1111/j.1365-3040.2010.02153.x.
- 760 54. Arneth, A.; Lloyd, J.; Šantrůčková, H.; Bird, M.; Grigoryev, S.; Kalaschnikov, Y. N.; Gleixner, G.; Schulze,
761 E.D. Response of central Siberian Scots pine to soil water deficit and long-term trends in atmospheric CO_2
762 concentration. *Glob. Biogeochem. Cycles* **2002**, *16*, 1005, DOI: 10.1029/2000GB001374.
- 763 55. Andreu-Hayles, L.; Planells, O.; Gutiérrez, E.; Muntan, E.; Helle, G.; Anchukaitis, K.J.; Schleser, G.H. Long
764 tree-ring chronologies reveal 20th century increases in water-use efficiency but no enhancement of tree
765 growth at five Iberian pine forests. *Glob. Chang. Biol.* **2011**, *17*, 2095–2112, DOI: 10.1111/j.1365-
766 2486.2010.02373.x.

- 767 56. Barbour, M.M. Stable oxygen isotope composition of plant tissue: a review. *Funct. Plant Biol.* **2007**, *34*, 83–
768 94, DOI: 10.1071/FP06228.
- 769 57. Feichtinger, L.M.; Siegwolf, R.T.W.; Gessler, A.; Buchmann, N.; Lévesque, M.; Rigling, A. Plasticity in gas-
770 exchange physiology of mature Scots pine and European larch drive short- and long-term adjustments to
771 changes in water availability. *Plant Cell Environ.* **2017**, *40*, 1972–1983, DOI: 10.1111/pce.13008.
- 772 58. Camarero, J.J.; Fernández-Pérez, L.; Kirilyanov, A.V.; Shestakova, T.A.; Knorre, A.A.; Kukarskih, V.V.;
773 Voltas, J. Minimum wood density of conifers portrays changes in early season precipitation at dry and cold
774 Eurasian regions. *Trees* **2017**, *31*, 1423–1437, DOI: 10.1007/s00468-017-1559-x.
- 775 59. Andreu, L.; Planells, O.; Gutiérrez, E.; Helle, G.; Schleser, G.H. Climatic significance of tree-ring width and
776 $\delta^{13}\text{C}$ in a Spanish pine forest network. *Tellus B* **2008**, *60*, 771–781, DOI: 10.1111/j.1600-0889.2008.00370.x.
- 777 60. Gessler, A.; Brandes, E.; Buchmann, N.; Helle, G.; Rennenberg, H.; Barnard, R.L. Tracing carbon and oxygen
778 isotope signals from newly assimilated sugars in the leaves to the tree-ring archive. *Plant Cell Environ.* **2009**,
779 *32*, 780–795, DOI: 10.1111/j.1365-3040.2009.01957.x.
- 780 61. Sarris, D.; Siegwolf, R.; Körner, C. Inter- and intra-annual stable carbon and oxygen isotope signals in
781 response to drought in Mediterranean pines. *Agr. Forest Meteorol.* **2013**, *168*, 59–68, DOI:
782 10.1016/j.agrformet.2012.08.007.
- 783 62. Eilmann B.; Zweifel R.; Buchmann N.; Fonti P.; Rigling A. Drought-induced adaptation of the xylem in
784 Scots pine and pubescent oak. *Tree Physiol.* **2009**, *29*, 1011–1020, DOI: 10.1093/treephys/tpp035.
- 785 63. Fernández de Uña, L.; Cañellas, I.; Gea-Izquierdo, G. Stand competition determines how different tree
786 species will cope with a warming climate. *PLoS One* **2015**, *10*, e0122255, DOI: 10.1371/journal.pone.0122255.
- 787 64. Lévesque, M.; Rigling, A.; Bugmann, H.; Webera, P.; Branga, P. Growth response of five co-occurring
788 conifers to drought across a wide climatic gradient in Central Europe. *Agric. For. Meteorol.* **2014**, *197*, 1–12,
789 DOI: 10.1016/j.agrformet.2014.06.001.
- 790 65. Saurer, M.; Spahni, R.; Frank, D.C.; Joos, F.; Leuenberger, M.; Loader, N.J.; McCarroll, D.; Gagen, M.;
791 Poulter, B.; Siegwolf, R.T.W.; Andreu-Hayles, L.; Boettger, T.; Dorado Liñán, I.; Fairchild, I.J.; Friedrich, M.;
792 Gutiérrez, E.; Haupt, M.; Hiltunen, E.; Heinrich, I.; Helle, G.; Grudd, H.; Jalkanen, R.; Levanič, T.;
793 Linderholm, H.W.; Robertson, I.; Sonninen, E.; Treydte, K.; Waterhouse, J.S.; Woodley, E.J.; Wynn, P.M.;
794 Young, G.H.F. Spatial variability and temporal trends in water-use efficiency of European forests. *Glob.*
795 *Chang. Biol.* **2014**, *20*, 332–336, DOI: 10.1111/gcb.12717.
- 796 66. Zhang, X.; Liu, X.; Zhang, Q.; Zeng, X.; Xu, G.; Wu, G.; Wang, W. Species-specific tree growth and intrinsic
797 water-use efficiency of Dahurian larch (*Larix gmelinii*) and Mongolian pine (*Pinus sylvestris* var. *mongolica*)
798 growing in a boreal permafrost region of the Greater Hinggan Mountains, Northeastern China. *Agric. For.*
799 *Meteorol.* **2018**, *248*, 145–155, DOI: 10.1016/j.agrformet.2017.09.013.
- 800 67. Li, D.; Fang, K.; Li, Y.; Chen, D.; Liu, X.; Dong, Z.; Zhou, F.; Guo, G.; Shi, F.; Xu, C.; Li, Y. Climate, intrinsic
801 water-use efficiency and tree growth over the past 150 years in humid subtropical China. *PLoS One* **2017**,
802 *12*, e0172045, DOI: 10.1371/journal.pone.0172045.
- 803 68. Linares, J.C.; Delgado-Huertas, A.; Camarero, J.J.; Merino, J.; Carreira, J.A. Competition and drought limit
804 the water-use efficiency response to rising atmospheric CO₂ in the Mediterranean fir *Abies pinsapo*. *Oecologia*
805 **2009**, *161*, 611–624, DOI: 10.1007/s00442-009-1409-7.
- 806 69. Maseyk, K.; Hemming, D.; Angert, A.; Leavitt, S.W.; Yakir, D. Increase in water-use efficiency and
807 underlying processes in pine forests across a precipitation gradient in the dry Mediterranean region over
808 the past 30 years. *Oecologia* **2011**, *167*, 573–585, DOI: 10.1007/s00442-011-2010-4.
- 809 70. Peñuelas, J.; Canadell, J.G.; Ogaya, R. Increased water-use efficiency during the 20th century did not
810 translate into enhanced tree growth. *Glob. Ecol. Biogeogr.* **2011**, *20*, 597–608, DOI: 10.1111/j.1466-
811 8238.2010.00608.x.
- 812 71. Battipaglia G.; De Micco V.; Brand W. A.; Saurer M.; Aronne G.; Linke P.; Cherubini, P. Drought impact on
813 water use efficiency and intra-annual density fluctuations in *Erica arborea* on Elba (Italy). *Plant Cell Environ.*
814 **2014**, *37*, 382–391, DOI: 10.1111/pce.12160.
- 815 72. Moreno-Gutiérrez, C.; Battipaglia, G.; Cherubini, P.; Delgado Huertas, A.; Querejeta, J.I. Pine afforestation
816 decreases the long-term performance of understorey shrubs in a semi-arid Mediterranean ecosystem: a
817 stable isotope approach. *Funct. Ecol.* **2015**, *29*, 15–25, DOI: 10.1111/1365-2435.12311.
- 818 73. Rehfeldt, G.E.; Tchebakova, N.M.; Parfenova, Y.I.; Wykoff, W.R.; Kuzmina, N.A.; Milyutin, L.I. Intraspecific
819 responses to climate in *Pinus sylvestris*. *Glob. Chang. Biol.* **2011**, *8*, 912–929, DOI: 10.1046/j.1365-
820 2486.2002.00516.x.

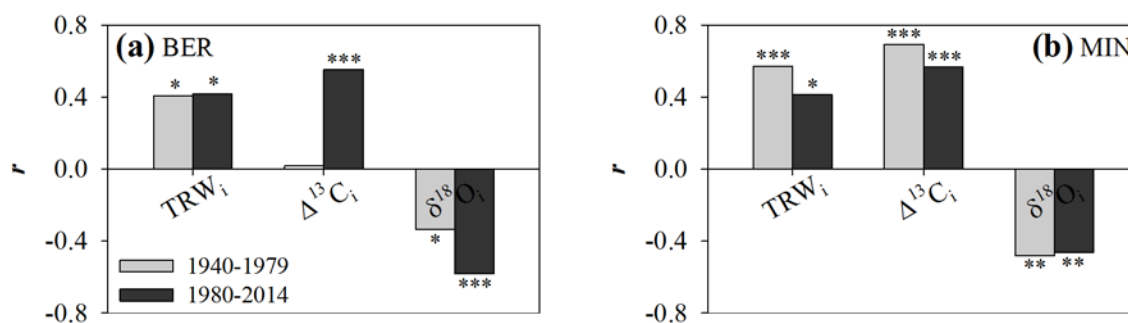
- 821 74. Fleischer, K.; Wårlind, D.; van der Molen, M.K.; Rebel, K.T.; Arneth, A.; Erisman, J.W.; Wassen, M.J.; Smith,
822 B.; Gough, C.M.; Margolis, H.A.; Cescatti, A.; Montagnani, L.; Arain, A.; Dolman, A. J. Low historical
823 nitrogen deposition effect on carbon sequestration in the boreal zone. *J. Geophys. Res.* **2015**, *120*, 2542–2561,
824 DOI: 10.1002/2015JG002988.
- 825 75. Rossi, S.; Deslauriers, A.; Gričar, J.; Seo, J.W.; Rathgeber, C.B.K.; Anfodillo, T.; Morin, H.; Levanic, T.; Oven,
826 P.; Jalkanen, R. Critical temperatures for xylogenesis in conifers of cold climates. *Glob. Ecol. Biogeogr.* **2008**,
827 *17*, 696–707, DOI: 10.1111/j.1466-8238.2008.00417.x.
- 828 76. Frank, D. C.; Poulter, B.; Saurer, M.; Esper, J.; Huntingford, C.; Helle, G.; Treydte, K.; Zimmermann, N. E.;
829 Schleser, G. H.; Ahlström, A.; Ciais, P.; Friedlingstein, P.; Levis, S.; Lomas, M.; Sitch, S.; Viovy, N.; Andreu-
830 Hayles, L.; Bednarz, Z.; Berninger, F.; Boettger, T.; D'Alessandro, C. M.; Daux, V.; Filot, M.; Grabner, M.;
831 Gutiérrez, E.; Haupt, M.; Hiltunen, E.; Jungner, H.; Kalela-Brundin, M.; Krapiec, M.; Leuenberger, M.;
832 Loader, N. J.; Marah, H.; Masson-Delmotte, V.; Pazdur, A.; Pawelczyk, S.; Pierre, M.; Planells, O.; Pukiene,
833 R.; Reynolds-Henne, C. E.; Rinne, K. T.; Saracino, A.; Sonninen, E.; Stievenard, M.; Switsur, V. R.;
834 Szczepanek, M.; Szychowska-Krapiec, E.; Todaro, L.; Waterhouse, J. S.; Weigl, M. Water-use efficiency and
835 transpiration across European forests during the Anthropocene. *Nat. Clim. Chang.* **2015**, *5*, 579–584, DOI:
836 10.1038/nclimate2614.
- 837 77. Martínez-Sancho, E.; Dorado-Liñán, I.; Gutiérrez-Merino, E.; Matiu, M.; Helle, G.; Heinrich, I.; Menzel, A.
838 Increased water-use efficiency translates into contrasting growth patterns of Scots pine and sessile oak at
839 their southern distribution limits. *Glob. Chang. Biol.* **2017**, accepted, DOI: 10.1111/gcb.13937.
- 840 78. Körner, C. Paradigm shift in plant growth control. *Curr. Opin. Plant Biol.* **2015**, *25*, 107–114, DOI:
841 10.1016/j.pbi.2015.05.003.



© 2017 by the authors. Submitted for possible open access publication under the terms and conditions of the Creative Commons Attribution (CC BY) license (<http://creativecommons.org/licenses/by/4.0/>)

846 **Supplementary material**

847



848

849

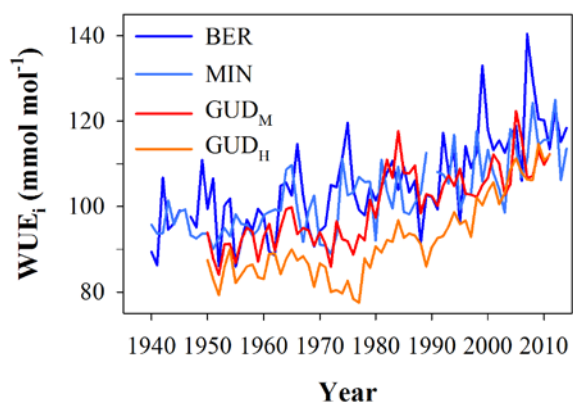
850

851

852

853

Figure S1. Changes in tree responses to seasonal drought stress for BER (a) and MIN (b) over the two halves of the study period (1940–1979 and 1980–2014). The relationships with climate are based on bootstrapped correlations between indexed tree-ring data (TRW_i, Δ¹³C_i and δ¹⁸O_i) corresponding to each site and May–August Standardized Precipitation-Evapotranspiration Index (SPEI). Asterisks denote significance at: *, $P < 0.05$; **, $P < 0.01$; ***, $P < 0.001$.



854

855

856

857

Figure S2. Long-term evolution of intrinsic water-use efficiency (WUE_i) of four Scots pine stands located in the forest-steppe zone of Central Siberia (BER, cold-dry; MIN, cold-moist) and in sub-Mediterranean Eastern Spain (GUD_L , warm-dry; GUD_H , warm-moist).

858 **Table S1.** Significance of fixed effects of linear mixed models with intrinsic water-use
 859 efficiency (WUE_i) explained as a function of Region (Central Siberia, Eastern Spain), Condition
 860 (dry, moist), atmospheric CO₂ concentration (C_a) and growing season water deficit (WD; potential
 861 evapotranspiration exceeding precipitation). Significant effects are indicated as follows: *, *P* < 0.05;
 862 **, *P* < 0.01; ***, *P* < 0.001. Abbreviation: DF, degrees of freedom.

Fixed effect	DF (numerator)	DF (denominator)	F-value	P-value
Region	1	163	0.03	0.857
Condition	1	163	5.43	0.021*
Region × Condition	1	163	16.14	<0.001***
C _a	1	163	140.49	<0.001***
C _a × Region	1	163	0.06	0.799
C _a × Condition	1	163	4.21	0.042*
C _a × Region × Condition	1	163	17.32	<0.001***
WD	1	163	38.23	<0.001***
WD × Region	1	163	9.40	0.003**
WD × Condition	1	163	0.08	0.773
WD × Region × Condition	1	163	0.51	0.476

863

864 **Table S2.** Significance of fixed effects of linear mixed models with basal area increment
 865 (logBAI) explained as a function of Region (Central Siberia, Eastern Spain), Condition (dry, moist)
 866 and intrinsic water-use efficiency (WUE_i). Significant effects are indicated as follows: *, $P < 0.01$;
 867 **, $P < 0.001$. Abbreviation: DF, degrees of freedom.

Fixed effect	DF (numerator)	DF (denominator)	F-value	P-value
Region	1	4220	13.06	<0.001***
Condition	1	4220	9.66	0.002**
Region × Condition	1	4220	0.21	0.646
WUE	1	4220	34.61	<0.001***
WUE × Region	1	4220	2.33	0.127
WUE × Condition	1	4220	11.04	<0.001***
WUE × Region × Condition	1	4220	0.09	0.771

868

869